LUND UNIVERSITY

Antenna Arrays for Dual-Frequency Harmonic Radar Application

Master's Thesis Report

By

Mohammad Zafar Mohammad and Venkatesh Raja

Supervisor: Docent. Anders J Johansson

Examiner: Professor Buon Kiong Lau

Department of Electrical and Information Technology
Faculty of Engineering, LTH, Lund University
SE-221 00 Lund, Sweden.

2023

Abstract

The aim of this thesis is to design two patch antenna arrays for dual-frequency harmonic radar application, one for the transmitter and the other for the receiver. The arrays are used to track the Bogong moth that migrates from the countryside to the Australian Alps during spring. The tracking is done at the radar by operating the transmitter at one frequency and the receiver at twice the frequency. A transponder is attached to the target which doubles the frequency of the signal received from the transmitter before sending the signal back to the receiver.

The antenna arrays at the radar are designed with the ISM band (unlicensed spectrum) of 5.8GHz for the transmitter and 11.6GHz for the receiver. Coupling and polarization play a major role in the patch antenna array design and these aspects are studied in this thesis. Based on the compatibility in the radar system the maximum allowed size of the antenna arrays should be less than or equal to 200×300mm. We have chosen RT/duroid 5880 substrate for both the transmitter and receiver antenna arrays with the permittivity of 2.20. Based on a previous study, at 5.8GHz we are supposed to get a gain of 20dBi at the transmitter array and 26dBi at the receiver array. Also, the bandwidth of the system is expected to be 50MHz. According to the planar array the aperture efficiency should be between 0.6 to 0.8 for the antenna arrays. We used FEKO, an electromagnetic simulation software, to design the antenna arrays. An edge port is used in the simulation as a source of power supply for the antenna arrays.

Upon designing the antenna arrays in the simulation software, various parameters have been examined. On that note, we obtained acceptable reflection coefficient, input impedance, and voltage standing wave ratio (VSWR). The simulated bandwidth, for the VSWR of less than 1.5, is verified in experiment. We used an SMA (Sub Miniature version A) connector for both the antenna arrays in the fabrication. We achieved a simulated gain of 15dBi at the transmitter array and 16dBi at the receiver antenna array.

Popular Science Summary

In Australia, billions of Bogong moths migrate from the countryside to the Australian Alps due to the unbearable hot weather. They migrate during the spring from different parts of the country, and they travel along thousands of kilometres and stay in the Alps for four months and then they return to their places of origin after the hot weather.

It has always been a mystery for scientists regarding how these moths travel a long way and settle down in the Alps together for several months. In order to solve this mystery, some scientists decide to track the moths using a radar system which monitors their movement. Practically, it is not possible to track all the moths, so the initial idea is to track a thousand of them using a miniature diode placed on each of their bodies.

The radar system which will be used for the tracking has a transmitter and a receiver antenna array. These arrays operate in different frequencies, the transmitter antenna array operates in one frequency and the receiver antenna array operates in another frequency. Thus, a harmonic radar is used such that the transmitted signal frequency is doubled by the transponder at the target and the return signal is received at a different frequency at the receiver array.

This thesis deals with the design of the antenna arrays and the techniques used for designing the antenna. The final design of fabricated antenna arrays is shown in the figures below.
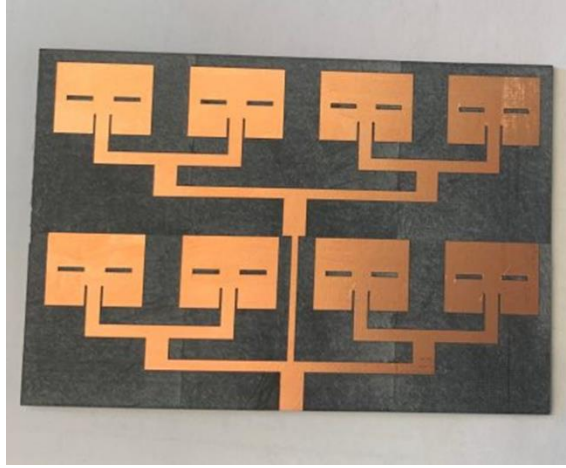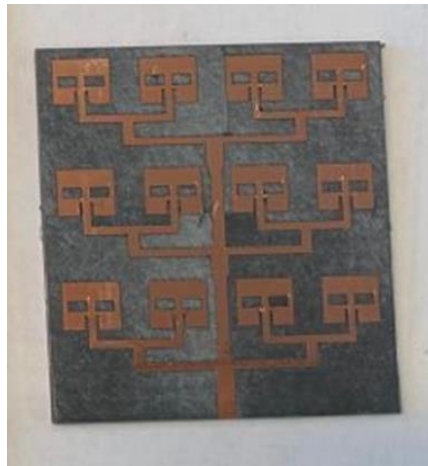
Figure A: Final design of transmitter array

Figure B: Final design of receiver array

Acknowledgements

We are grateful to our supervisor Anders J Johansson for his unwavering support, guidance, and insights throughout the master's thesis. We would like to also thank the postdocs in our department Casimir and Johan for helping us with a few parts of the thesis. We also thank our examiner Buon Kiong Lau for his valuable feedback and insights. It is a great opportunity to study at LTH in Lund University with intelligent minds and meet people from all over the world. Our experiences will help us to get a head start in our careers.

Finally, I Venkatesh Raja would like to thank my mother, my father, my sister, God, and my project partner for their immense support all through the hurdles of my studies.

I Mohammad Zafar Mohammad, would like to thank God, my father, my mother, my project partner, and a special thank my wife Beheshta Ataei who has encouraged and helped me a lot during my studies.

Contents

List of Figures

List of Tables

Chapter **1**
Introduction

_____

This thesis aims to design antenna arrays for a dual-frequency harmonic radar application. Harmonic radar is used to find the location of small objects from a long distance. They operate in dual frequency, that is, the transmitter antenna is allocated to work in one frequency and the receiver antenna a different frequency. This is done to avoid reflections from the surrounding environment, and to reduce the interference between the transmitter and receiver signal. We have the antenna array at one end (i.e., in the drone) and a nonlinear element at the target of interest (i.e., on the moth) such as a diode, powered by the transmitted electromagnetic wave of the radar. When an electromagnetic signal is sent from the transmitter antenna at one frequency to the target, we receive a signal with a harmonic frequency reflected from the target. We use the harmonic frequency radar technique to make the radar signal resistant to objects in the environment. The transmitted signals encountering the objects in the channel will have the same frequency as the transmitted signal and having a different received signal frequency helping us segregate the received signal from the clutters. Thus, the reflected signal from the target will be received without channel clutters at the harmonic frequency. The radar system measures the time difference between transmitted and received signals to find the location of the Bogong moth. This radar system will be used to track the location of the Bogong moth in Australia. The size of the antenna is a major concern in this project since we will mount the antenna in a flying drone. The antenna should be as small as possible, but without affecting the performance of the antenna array.

1.1.   Background Study and Motivation

In Australia, billions of Bogong moths from different parts of the country migrate every year for hundreds of kilometres. This occurs in the spring when they migrate to the Australian Alps, in search of a cold place since

they cannot tolerate the warm weather. The Bogong moths return to their original places after spending almost four months in the mountains. It is interesting for researchers is to study how moths travel hundreds of kilometres and find a place where they have never been before. It's been a challenge for researchers to find the moths and study how they navigate, because of their hibernation nature to hide under trees, small opening places in the mountains, among others.

To find the location of moths, researchers propose to use a low-power harmonic radar system. This system includes a drone equipped with a radar whose transmitter and receiver antennas consist of patch antenna arrays. The antennas should be as small as possible since they are mounted on a flying drone, which should be energy efficient. A miniature diode is used on the Bogong moth which doubles the received frequency from the transmitter antenna and sends it to the receiver radar antenna. The antenna parameters for this application have been identified and a patch array should then be designed using an electromagnetic simulation software.
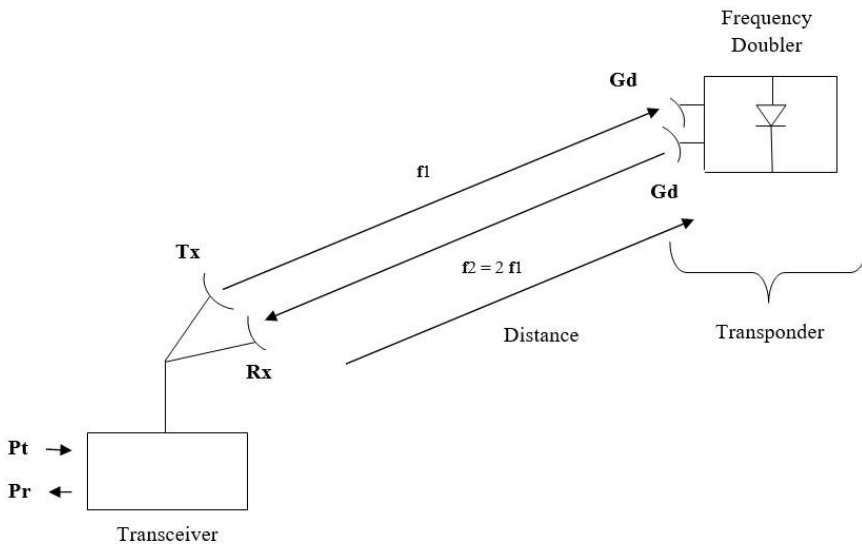
Figure 1.1. Block diagram of transceiver and transponder.

where
- Gd = Gain at the transponder
- Tx = Transmitter antenna array
- Rx = Receiver antenna array
- F = Frequency
- Pt = Transmitted power
- Pr = Received power

The above figure gives an overview setup of the harmonic radar system. However, in our thesis, we will be concentrating on the transceiver part, especially on the methods followed in designing the transmitter and receiver antenna arrays.

1.2. Thesis Objective

The main objective of this thesis is to design a transmitter and receiver antenna array for a harmonic radar application. The steps to achieve this are as follows,

- The first step of this thesis is to model the antenna in a licensed spectrum (ISM band) at 5.8GHz at the transmitter and 11.6GHz at the receiver. Analysing the type of the substrate, permittivity, and the feeding technique to be used plays a major role in contributing to the performance of the antenna.

- Calculate the dimensions of the microstrip antenna in MATLAB. Then, design the antenna and simulate them in FEKO, an electromagnetic simulation software.

- Design different antenna models namely, a microstrip antenna, a microstrip antenna placed with a passive resonator, and a slotted microstrip antenna. Validate that the antenna design with a slotted patch can indeed achieve a higher bandwidth. The bandwidth is given by the frequency range where the voltage standing wave ratio (VSWR) parameter is less than 1.5.

- Design the antenna arrays for both the transmitter and receiver with a size constraint of 200×300mm.

- Finally, compare the simulation results with the requirements of the thesis and check them with theoretical values.

1.3. Organization

We have divided our report into 8 chapters, starting from this introductory one. The next chapter is about explaining the key parameters used in our thesis. Chapter 3 details the equations and mathematical calculations for designing a microstrip patch antenna element, and the simulation results are also checked. Chapter 4 shows the different approaches used to enhance the performance of the patch antenna. It also makes a comparison between the mathematical calculations and simulation results for different patch antenna designs. Chapter 5 presents the techniques used in designing the transmitter antenna array and the following Chapter 6 deals with the same aspects for the receiver antenna array. Chapter 7 presents some measured results obtained from the designed patch arrays that were fabricated for experimental validation. Finally, the report ends with Chapter 8, which discusses the results obtained and concludes with some possible future work.

Chapter 2

Antenna Parameters and Measurements

In this chapter, we will introduce the basic antenna parameters used in the design and measurement of patch antennas. Nowadays, most of the wireless communication systems require antennas with high performance, light weight, low profile, planar structure, and ease of integration with active devices. Microstrip antenna is a suitable antenna among the antennas which meet these requirements. According to [1]: "Microstrip antenna is also known as patch antenna and it is a popular antenna well suitable for systems to be mounted on airborne platforms, like synthetic-aperture radar (SAR) and scatterometers".

2.1. Reflection Coefficient

Reflection coefficient describes the amount of electromagnetic wave that is reflected in the transmission medium due to impedance discontinuity. It is equal to the ratio of the amplitude of the reflected wave to the incident wave.

Reflection coefficient is also called return loss, although the latter is given in positive values when expressed in the decibel (dB) scale. Reflection coefficient can be expressed in terms of the load and feeder characteristic impedances as:

$$\Gamma = \frac{|Z_L - Z_o|}{|Z_L + Z_o|}, \tag{2.1}$$

where
Γ = reflection coefficient
Z_L = load impedance
Z_0 = feeder characteristic impedance

2.2. Impedance

Impedance is defined as the effective resistance of an electric circuit or component to an alternating current, which is a combined effect of ohmic resistance and reactance.

In antenna design, impedance matching plays a vital role for the system to work consistently. In impedance matching, the input impedance of a load (or the output impedance of the source) is designed so that the output (or input power) of the system can be increased by minimizing the reflection.

For real-valued impedances, the maximum power transfer is obtained when:

$$Z_0 = Z_L ,$$
(2.2)

where
Z_0 = source impedance
Z_L = load impedance

2.3. VSWR

VSWR stands for voltage standing wave ratio, and it is also stated as SWR (standing wave ratio). It is the amount of power reflected from the antenna (in the transmitter antenna case) since it is a function of the reflection coefficient. If reflection coefficient is denoted by Γ then the VSWR is denoted by:

$$VSWR = \frac{(1+|\Gamma|)}{(1-|\Gamma|)}$$
(2.3)

VSWR is always a real number, and it is positive. Generally, the antenna performance is improved with a smaller VSWR. It is commonly to define an antenna's operating bandwidth by VSWR = 2:1, which means that the frequency range where VSWR is less than 2. This means that the antenna is operating efficiently within this frequency range.

2.4. Gain

The gain of an antenna is a key performance parameter of the antenna. The combination of antenna directivity and electrical efficiency can be referred to as gain. It is defined by:

Antenna Gain = Directivity × Antenna Efficiency   **(2.4)**

In a transmitter antenna, the gain represents the conversion of input power to radio waves in the desired direction, whereas in a receiver antenna, it is the conversion of radio waves arriving from a specified direction to the received power.

The gain of an antenna is measured in dBi (decibel isotropic) or dBd (decibel dipole). When the energy is radiated equally in all directions into an imaginary sphere surrounding a point source then it is called an isotropic radiator. The measure of dBi uses the isotropic radiator as the reference case. A dipole (omnidirectional in the azimuth plane for a vertical dipole) antenna has 2.15dB more gain than an isotropic antenna in the azimuth plane. When a dipole antenna is vertically oriented, the gain in the azimuth plane comes at the expense of that in the region above and below the antenna. Its antenna pattern seems like a donut. The measure of dBd refers to the antenna gain using a reference dipole antenna. As a result, the relationship between dBi and dBd can be represented as follows,

- dBi = dBd + 2.15
- dBd = dBi − 2.15

2.5. Directivity

Directivity is the measure of how directional the radiation pattern of an antenna is. In other words, it can be said to be the measure of the degree to which the radiation emitted is concentrated in a single direction. Directivity is also defined as an antenna receiving electromagnetic waves, and its directivity when receiving is equal to its directivity when transmitting.

Directivity = U_{max}/ U_{av}   **(2.5)**

where
U_{max} = maximum radiation intensity
U_{av} = average radiation intensity

When the directivity is higher for an antenna then it can be used in permanent networks like satellite television, wireless backhaul, etc. since they need to transfer information for a longer distance in a particular direction. If the antenna is radiating equally in all directions (i.e., theoretical isotropic antenna), then the directivity will be 0dB. For antennas used in mobile devices, which should be insensitive to the orientation of the devices, the directivity should be low.

2.6. Beamwidth

Beamwidth is basically a metric derived from the radiation pattern of an antenna. The beamwidth changes according to the design, orientation, frequency, and type of antenna used. "It may be measured in the horizontal or vertical plane and is the distance between two points where the power is less than half of the maximum" [2].

The beamwidth can be expressed in two different ways:

Half Power Beam Width (HPBW): "The half-power beamwidth is the angle between the half-power (-3dB) points of the main lobe when referenced to the peak effective radiated power of the main lobe" [3]**.** HPBW is considered to be very useful and can be related to the gain of an antenna.

First Null Beam Width (FNBW): FNBW can be found in the antenna radiation pattern between the null points of the main lobe. Measuring FNBW helps in obtaining an approximation of antenna interference, as it is a measure of the angular separation from the main beam.

Both HPBW and FNBW are illustrated below for a representative directional antenna pattern.
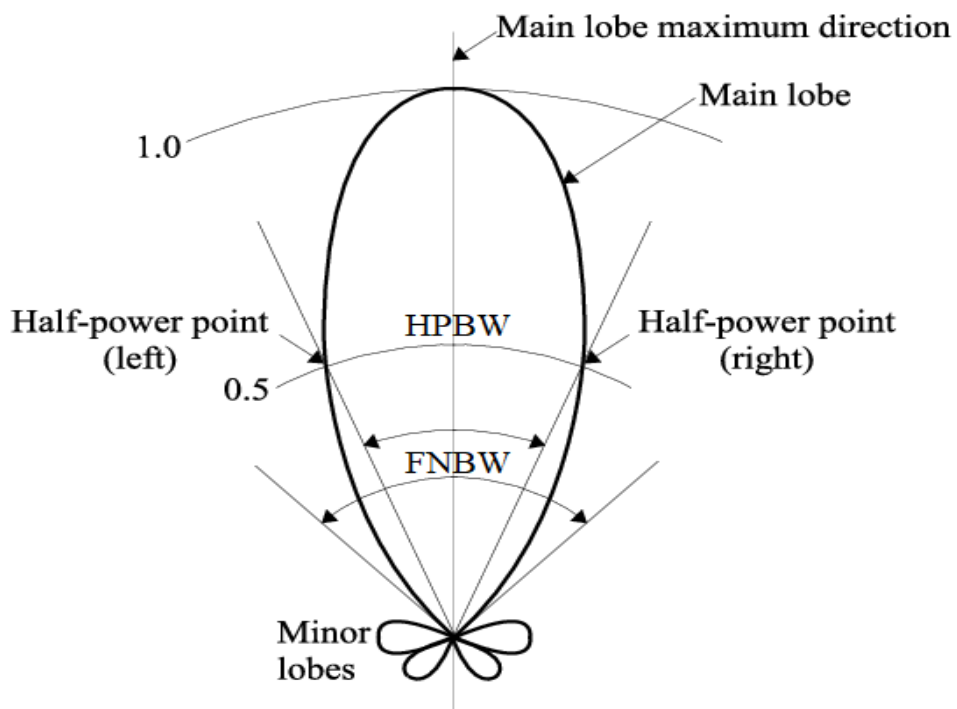
Figure 2.1: Illustration of HPBW and FNBW [4].

Chapter 3
Design of Rectangular Microstrip Patch Antenna

This chapter will guide you on how a patch antenna is being designed. The basic formulas and steps for the design are explained clearly to help readers to design their own patch antenna.

The microstrip patch antenna consists of two parts: a dielectric substrate with a ground plane is used as the base and a metallic patch is placed on top of the substrate. The substrate is a semi-conducting material with a permittivity value that contributes to the properties of the antenna.

Designing of the Rectangular Patch Antenna

The following steps are carried out for the theoretical calculations and design of a patch antenna,

3.1. Substrate for the Antenna

The thickness and the dielectric constant of the substrate play a major role in contributing to the performance of the antenna. Microstrip patch antennas can be designed using a wide range of substrate materials that possess mechanical, thermal, and electrical properties, which can be used either in planar or conformal antenna configurations. However, the dielectric constant tolerance control is still a challenge, especially for microwave and millimetre frequencies [5].

A thin substrate with a high dielectric constant is preferable for microwave circuit design as such a design often needs tightly bound fields to minimize mutual coupling and unwanted radiation. This choice also gives us a smaller element size but at the expense of efficiency and bandwidth. However, if the only aspect of the design to be evaluated is its antenna performance,

selecting a thick substrate with a lower dielectric constant is preferable. Loosely bound fields can radiate efficiently into space, which increases efficiency and bandwidth, but at the expense of larger element size [6]. In our antenna design, we have chosen Rogers RO4350B (with dielectric constant of 3.48 and loss tangent of 0.0037 at 10 GHz) for both the transmitter and receiver parts.

3.2. Theoretical Calculations for Patch Antenna Design

Once we are done with selecting the key parameters like the resonant frequency, dielectric constant, and the height of the substrate, we can move on to calculating the dimensions for the patch antenna.

Step 1: **Feeding Method**

Generally, there are different methods of feeding a microstrip patch antenna. They are divided into contacting or non-contacting methods. The microstrip feed and coaxial feed come under the contacting method since the RF power is fed directly to the radiating patch using a connecting element. On the other hand, the aperture coupled feed and proximity coupled feed come under the non-contacting method since electromagnetic coupling is utilized to transfer the power between the feed line and the radiating patch [7]. The feeding technique is important for a microstrip patch antenna since different excitation techniques give different bandwidth, reflection coefficient, impedance matching, beamwidth, VSWR, and radiation pattern. An illustration of different feeding techniques is shown in the figures below.
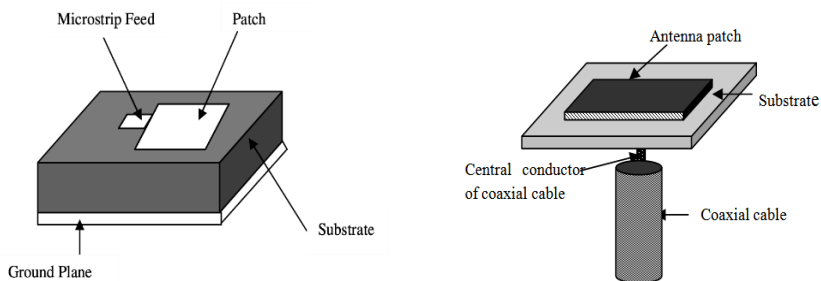
a. Microstrip line feed [8].   **b.** Coaxial probe feed [9].

Figure 3.1: Contacting feeding methods.

a. Proximity coupled feed.　　**b.** Aperture coupled feed.
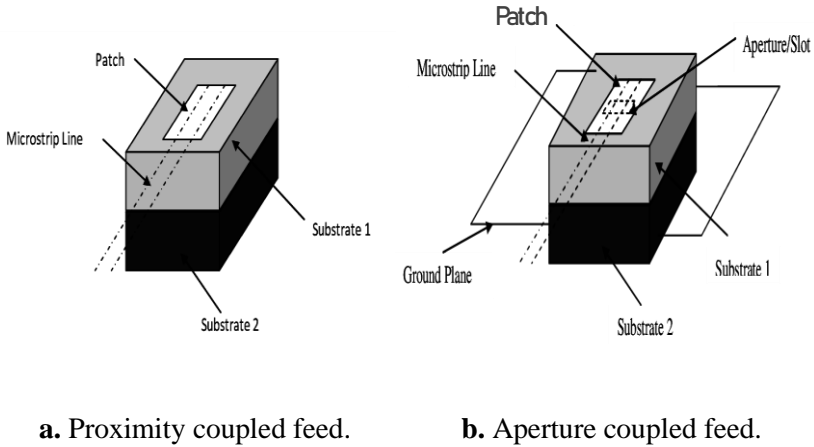
Figure 3.2: Non-contacting feeding methods [8].

All the feeding techniques have their own pros and cons. The non-contacting techniques give more bandwidth, and it is advantageous to reduce harmonic radiation of microstrip patch antenna implemented in a multilayer substrate and allows independent optimization of antennas and feed networks by using substrates of different thickness or permittivity. But the main disadvantage of these techniques is that the design and fabrication of the antenna are complicated. In contrast, in contacting techniques, the coaxial fed has the least bandwidth, and it is difficult to model.

Considering the practical design and manufacturing parameters needed for our project we found that the inset feed technique is apt, easy to fabricate, and simple in structure [7]. Thus, we chose the inset feed technique for our thesis. When the patch is fed through a source, the edge closer to the source has infinite impedance because of zero current at the open circuit edge, whereas at the middle of the patch, the impedance is zero because of maximum current at the patch centre. Hence, a 50Ω input impedance feed point is selected by moving it closer to the patch centre [6]. Therefore, in the inset feed technique the input impedance can be changed by choosing the feed point and by modifying the dimension of the patch. We have used both the inset feed technique and quarter wavelength transformer to perform the impedance matching in our thesis.

A quarter wavelength transformer, as shown in Fig. 3.3, has a transmission line that is a quarter of the wavelength, and it is used to match the input

impedance of the patch to 50Ω. The characteristic impedance of the quarter wavelength transformer is given by:

$$Z_C = \sqrt{Z_0 * Z_L} \; , \qquad\qquad\qquad (3.1)$$

where Z_C is the impedance of the quarter-wave transformer in a single patch antenna, and in an array, it is the characteristic impedance of the feed line [10].

λ/4

Z_0 $\qquad\qquad$ Z_1 $\qquad\qquad\qquad\qquad$ Z_R
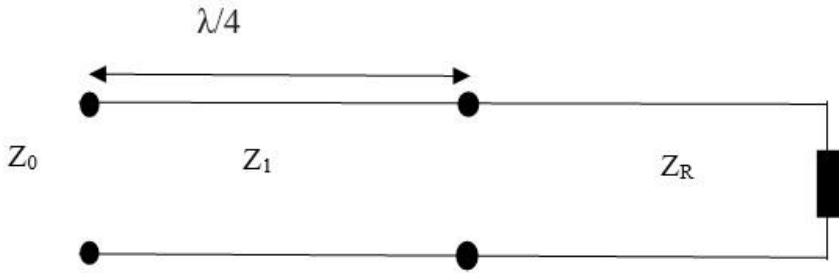
Figure 3.3: Single-section quarter wavelength transformer.

Once Z_C is found then the width of the feed line can be calculated by:

$$Z_C = \begin{cases} \dfrac{60}{\sqrt{\varepsilon_{reff}}} \ln\left[\dfrac{8h}{Wf} + \dfrac{Wf}{4h}\right] , \dfrac{Wf}{h} \le 1 \\[4mm] \dfrac{120\pi}{\sqrt{\varepsilon_{reff}} \left[\dfrac{Wf}{h} + 1.393 + 0.667 \ln\left(\dfrac{Wf}{h} + 1.444\right)\right]}, \dfrac{Wf}{h} > 1 \end{cases} , \qquad (3.2)$$

where Wf the width of the microstrip line and h is the thickness of the substrate.

The inset feed line's characteristic impedance depends on the width of the inset feed line. According to equation (3.2) the characteristic impedance will change inversely according to the change in inset width [6].

Step 2: **Length of the Patch** [10]

$$Lp = \frac{c}{(2f \sqrt{\varepsilon_{reff}})}$$ (3.3)

Step 3: **Width of the Patch** [10]

$$wp = \frac{c}{2*f} \sqrt{\frac{2}{(\varepsilon_r+1)}}$$ (3.4)

Step 4: **Effective Permittivity** [10]

$$\varepsilon_{reff} = \frac{(\varepsilon_r+1)}{2} \frac{(\varepsilon_r-1)}{2\sqrt{\frac{1}{1+\left(\frac{12h}{wp}\right)}}}$$ (3.5)

Step 5: **Length Extension** [10]

$$\Delta L = (0.412h) \frac{(\varepsilon_{reff}+0.3)\left(\frac{wp}{h}+0.26\right)}{(\varepsilon_{reff}-0.258)\left(\frac{wp}{h}+0.8\right)}$$ (3.6)

Step 6: **Determination of Inset Feed Depth (y_0)** [11]

y_0 indicates the position of the inset feed point where the input impedance is 50Ω.

$$R_{in}(y = y_0) = R_{in}(y = 0)\cos^{2\left(\frac{(\pi y_0)}{Lp}\right)}$$ (3.7)

And y_0 is equal to

$$y_0 = \frac{L_p}{\pi} \cos^{-1}\left(\sqrt{\frac{R_{in}(y=y_0)}{R_{in}(y=0)}}\right)$$ (3.8)

where R_{in} ($y = y_0$) is input impedance, or it is also known as resonant input impedance Z_{in}. This is usually 50Ω and R_{in} ($y = y_0$) is known as input

impedance at the edge of the patch. To calculate y_0 we need to know the resonant input resistance $R_{in}(y = 0)$ and it can be calculated [12].

Step 7: A good approximation of width of the substrate Ws [7]

$$ws = wp + 6 * h \tag{3.9}$$

Step 8: A good approximation of length of the substrate Ls [7]

$$ls = Lp + 6 * h \tag{3.10}$$

Thus, we have found all the parameters theoretically to design the patch antenna. It is noted that the above formulas can give a good approximation of the dimensions for the microstrip antenna, but these parameters may need to be fine-tuned for the simulation model. An illustration of the dimensions of the patch antenna with the quarter wavelength transformer is given in Fig. 3.4.
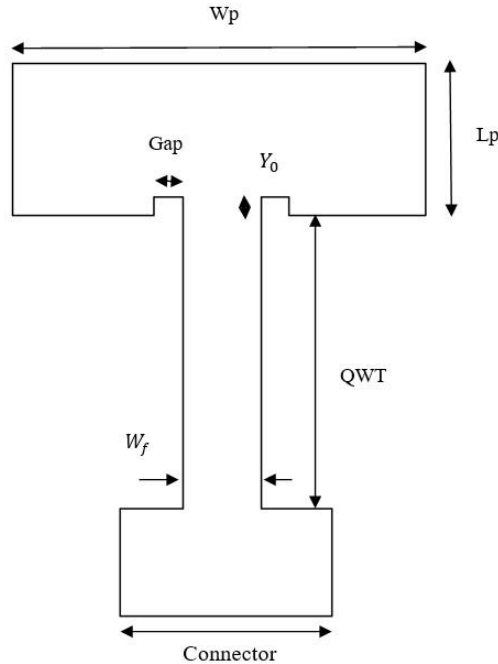
Figure 3.4: Quarter wavelength transformer with inset feed matching 50Ω for single patch.

The numerical values found for the transmitter patch antenna are shown below in Table 3.1.

Parameters	Values (mm)
Length of the patch	12.65
Width of the patch	16.94
Inset depth	3.67
Inset width	0.5
Length of quarter wavelength transformer	6.56
Width of quarter wavelength transformer	2.84

Table.3.1: Theoretical values for transmitter patch antenna obtained from the formulas.

In the same way, the values obtained for the receiver antenna from the formulas are shown in Table 3.2 below.

Parameters	Values (mm)
Length of the patch	6.51
Width of the patch	10.22
Inset depth	2.18
Inset width	0.5
Length of quarter wavelength transformer	4
Width of quarter wavelength transformer	1.11

Table.3.2: Theoretical values for receiver patch antenna obtained from the formulas.

3.3. Simulation and the Effect of Parameters

The above-calculated values are used in the latest version of FEKO, an electromagnetic simulation software. A model of the designed patch antenna is shown in Fig. 3.5.
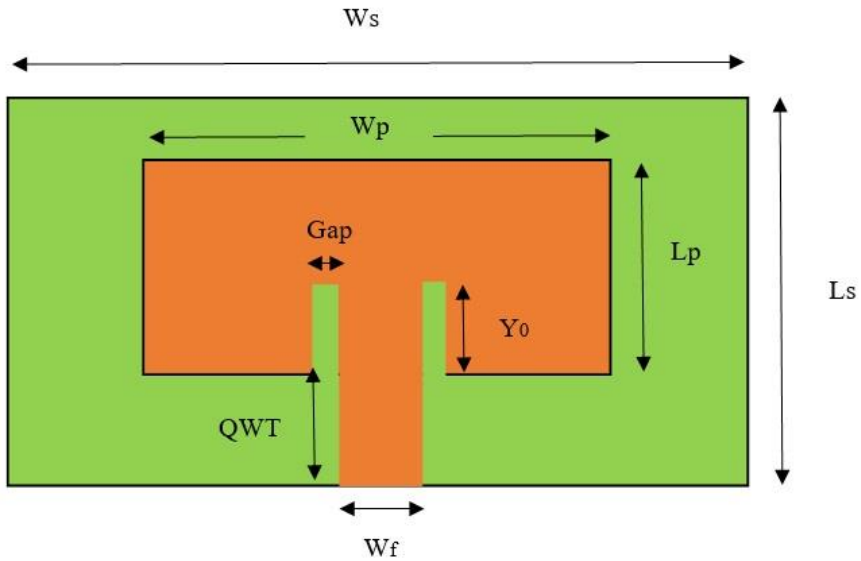
Figure 3.5: Model of the designed patch antenna.

where

- Ws = Width of the substrate
- Ls = Length of the substrate
- Wp = Width of the patch
- Lp = Length of the patch
- Y_0 = Inset depth
- Gap = Inset gap or width
- QWT= Quarter wavelength transformer
- Wf = Width of the feed

Length of the patch (Lp): Increasing/decreasing the patch length will decrease/increase the resonant frequency and the impedance (Z) according to the rule of thumb mentioned below. The impedance consists of two parts: real and imaginary parts. The real part of (Z) is known as the resistance and the imaginary part is called the reactance, which is zero at the resonant

frequency. Further, the reactance consists of capacitive reactance X_c and inductive reactance X_L, given by:

$$X_c = \frac{1}{2\pi f C}$$ (3.11)

$$X_L = 2\pi f L$$ (3.12)

where
- f = resonant frequency,
- C = capacitance of the capacitor,
- L = inductance of the inductor.

The reactance can be a negative (capacitive reactance) or positive (inductive reactance) value so by changing the resonant frequency the reactance will increase or decrease.

Width of the patch (Wp): Changing Wp will affect the gain, bandwidth, and frequency of the microstrip patch antenna. A higher Wp will give a higher bandwidth and gain, lower frequency, and the real part of the impedance will be decreased. But there is a limitation of changing the Wp.

Inset depth (Y_0): The input impedance is zero at the centre of the patch and higher at the edge so by increasing the Y_0 the feed point is going nearer to the centre, which results in a decrease of frequency and impedance.

In other word, Z is inversely proportional to the Y_0:

$$Z = \frac{1}{Y_0}$$ (3.13)

The other parameters like the length and width of the substrate, the length and width of the microstrip line also affect the resonant frequency, VSWR, impedance, etc.

During the simulations, the parameters are analysed and optimised according to our thesis requirements to get the necessary output. Because the calculated values from the formula are just the approximation of the parameter values, we cannot take them as true values for manufacturing in real-life. Thus, some values must be modified to get the expected results.

Below we have mentioned a few rules of thumb that we followed to optimise the parameters, they are [5]:

- When you change the length of the patch it influences the resonant frequency, i.e., when you increase the length of the patch then there will be a drop in the resonant frequency and vice versa.
- In the same way, when you change the inset depth, it influences the reflection coefficient, which means that when you decrease the inset depth, then you can see a poor reflection coefficient and a good one when you increase the inset depth.
- Also, other parameters like the length and width of the connector, and the quarter wavelength transformer contribute to the design and performance of the antenna.
- Having worked on the simulation and with some modified parameters, we then obtained good results for the reflection coefficient, VSWR, impedance, and gain.

Table 3.3 below shows the results obtained for the transmitter antenna after tuning the simulation model to meet the performance requirements.

Parameters	Values (mm)
Length of the patch	13.019
Width of the patch	16.443
Inset depth	4.079
Inset width	0.5
Length of Quarter wavelength transformer	6.564
Width of Quarter wavelength transformer	2.84

Table.3.3: Antenna parameters obtained for transmitter antenna from the simulation.

The final parameter values for the receiver antenna (after tuning the simulation model) are shown in Table 3.4 below.

Parameters	Values (mm)
Length of the patch	6.235
Width of the patch	8.471
Inset depth	1.743

Inset width	0.5
Length of Quarter wavelength transformer	2.717
Width of Quarter wavelength transformer	1.558

Table.3.4: Antenna parameters obtained for receiver antenna from the simulation.

3.4. Simulation Results

The simulation results of the gain, reflection coefficient, VSWR and impedance for both the transmitter and receiver patch antennas are illustrated in this section. The maximum gain is obtained from the polar plot.

3.4.1. Microstrip Transmitter Antenna

From the simulation, we obtained the different plots for the microstrip patch antenna. The results are shown in the following figures.
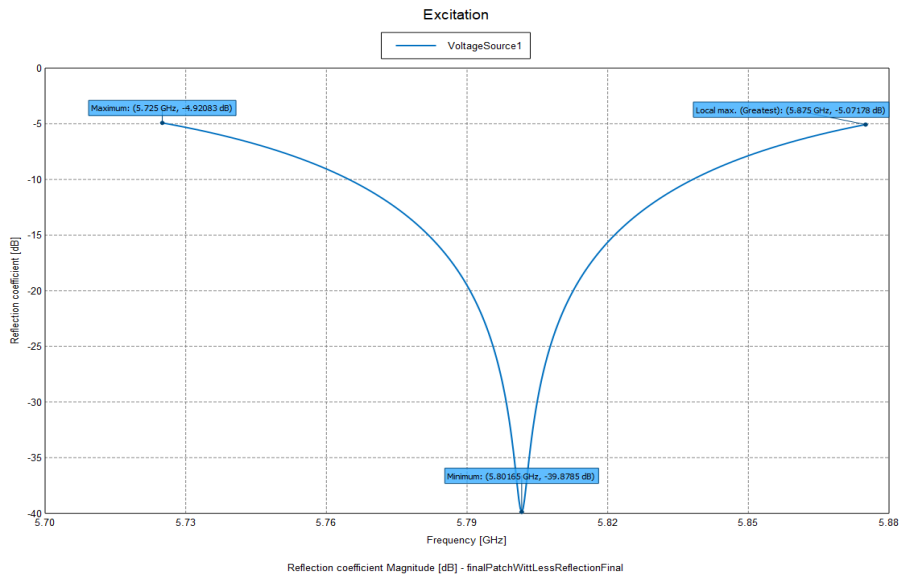
Figure 3.6: Reflection coefficient for single patch, with -39.87dB at 5.8GHz.
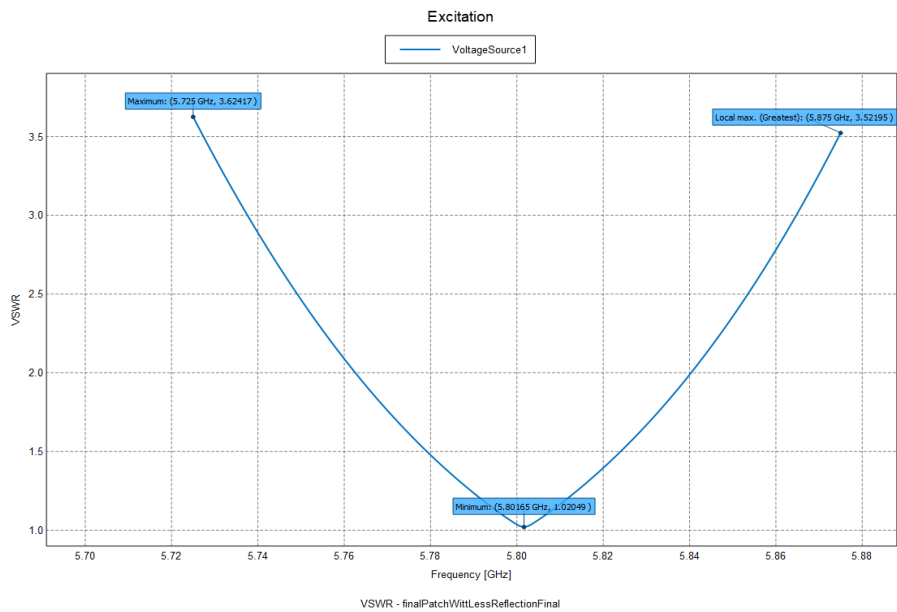
Figure 3.7: VSWR for single patch, with 1.02 at 5.8GHz.
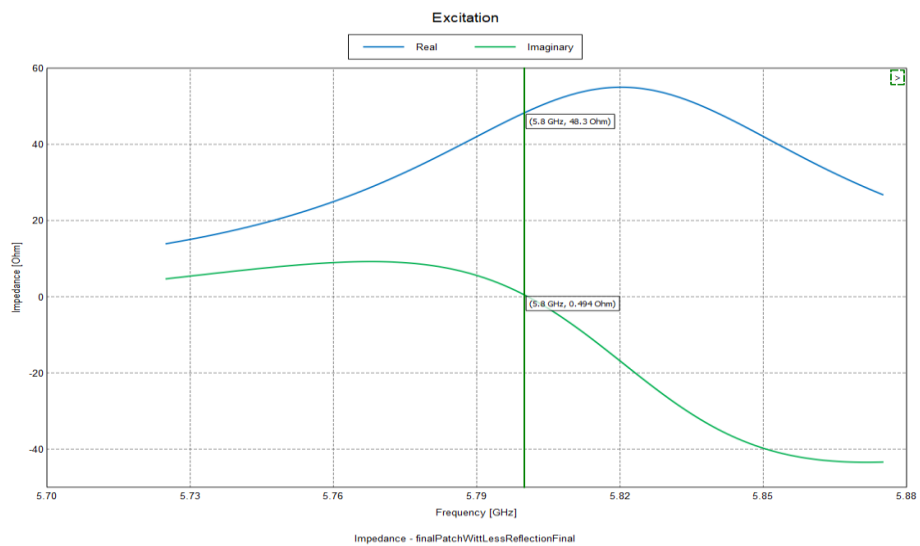
Figure 3.8: Real and imaginary parts of the impedance, with 48.3Ω in real part and 0.494Ω in imaginary part at 5.8GHz.
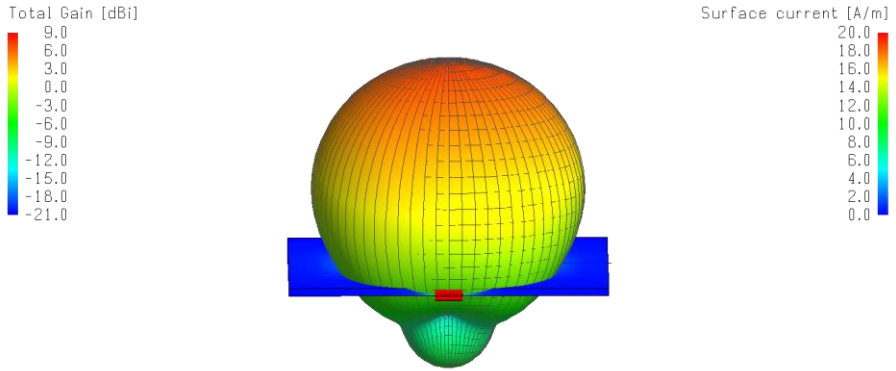
Figure 3.9: 3D gain pattern at resonant frequency of 5.8GHz, with maximum gain of 6.9dBi.
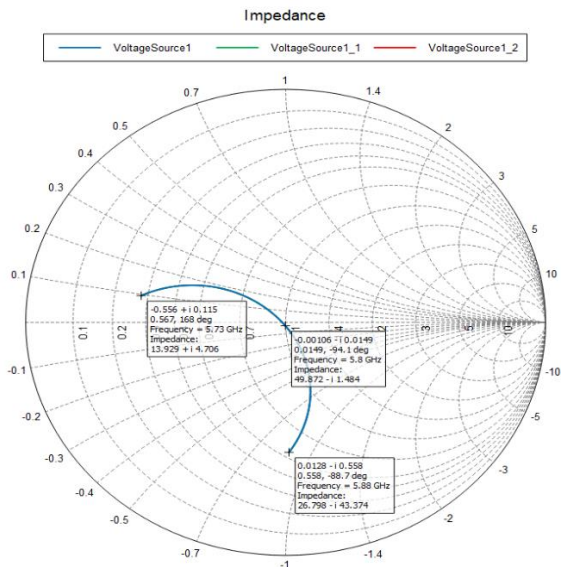
Figure 3.10: Smith chart showing the impedance trace between 5.73-5.88GHz.
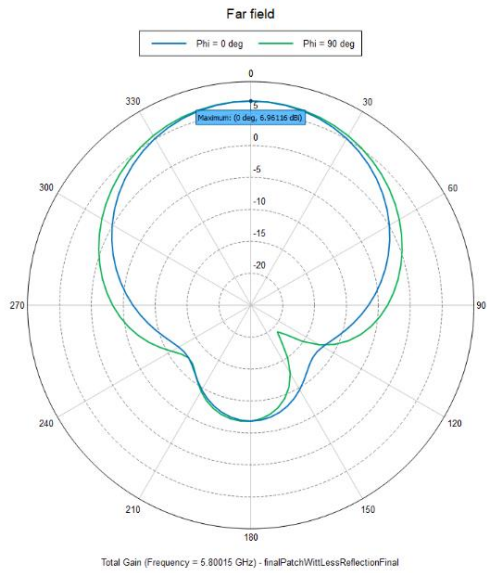
Figure 3.11: Polar plot showing the far field total gain at resonant frequency 5.8GHz in Z plane.

3.4.2. Microstrip Receiver Antenna

The results from the simulations for the receiver antenna are shown below.
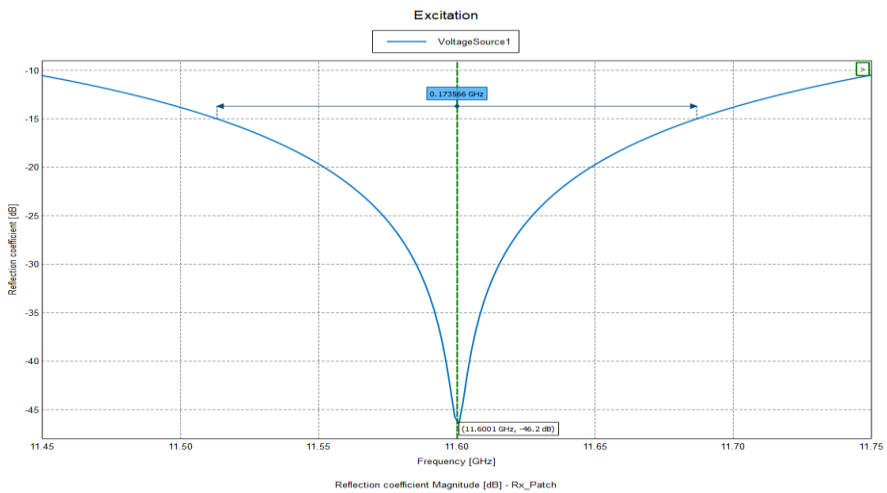
Figure 3.12: Reflection coefficient for single patch, with -46.2dB at 11.6GHz.
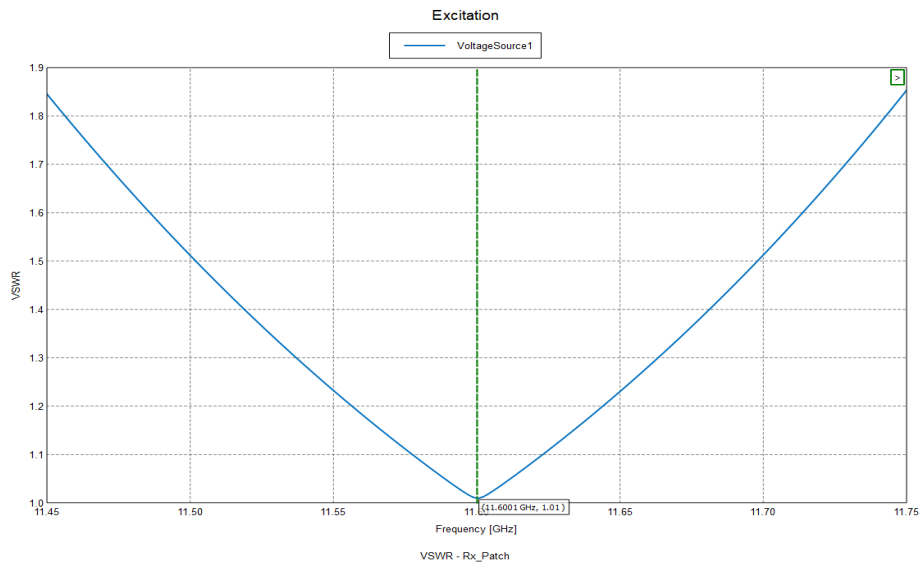
Figure 3.13: VSWR for single patch, with 1.01 at 11.6GHz.
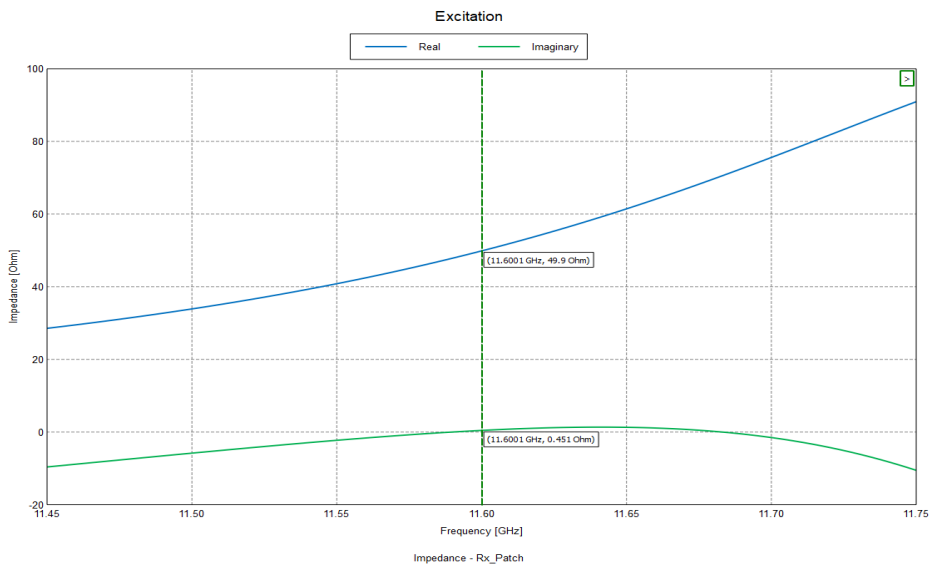
Figure 3.14: Real and imaginary parts of impedance, with 49.9Ω in real part and 0.451Ω in imaginary part at 11.6GHz.
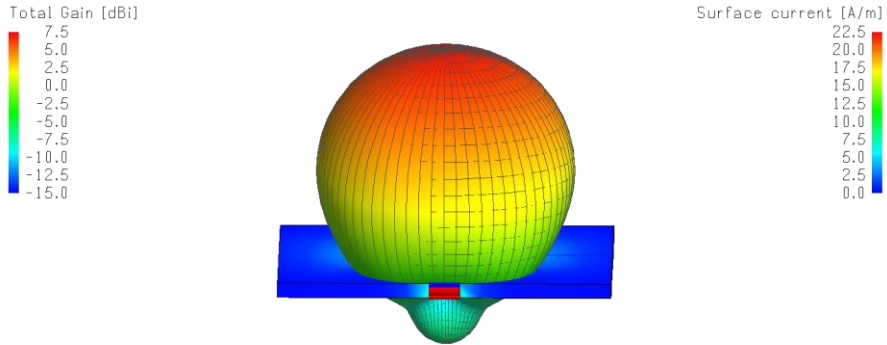
Figure 3.15: 3D gain pattern at resonant frequency of 11.6GHz, with maximum gain of 6.9dBi.
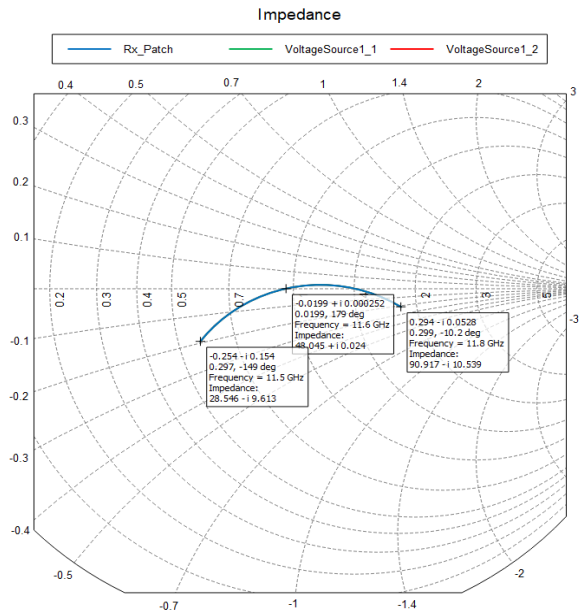
Figure 3.16: Illustration of zoomed in Smith chart showing the impedance trace in frequency range 11.5-11.8GHz.
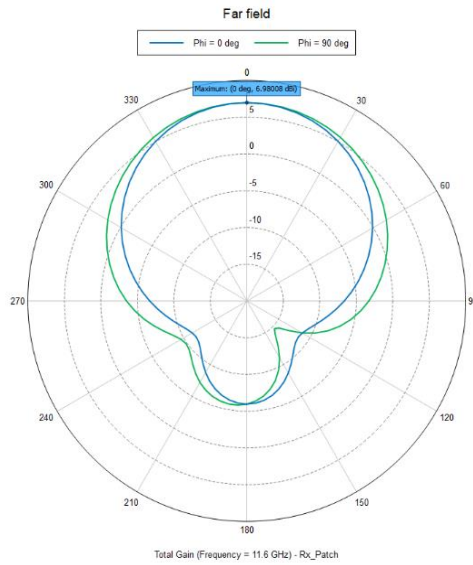
Figure 3.17: Polar plot showing the far field total gain at resonant frequency 11.6GHz in Z plane.

Chapter 4

Performance Enhancement Using Slotted Patch

_____

In this chapter, we will discuss the enhancement of the antenna performance using a slotted patch. Since the antennas are intended for a real propagation environment there is a high chance of the signals encountering obstacles. This will lead to fading of the signal. Therefore, we need better gain, reflection coefficient, etc. for the antenna mounted on the drone to have better efficiency in monitoring the tag on the Bogong moth. Also, the bandwidth of the radar system determines the range resolution for pulsed radars and on the delay bandwidth product for the FMCW radars [13]. The bandwidth also comes under the ISM bandwidth regulations, but the achieved antenna bandwidth is small and can be increased without breaking the regulation. So, we thought of increasing the bandwidth by adjusting the design of the antenna. We kept a threshold for the VSWR parameter to be less than 1.5 from which we can measure the bandwidth needed for our thesis. Thereby we used slots in the patch which will influence the gain, bandwidth, resonant frequency, and impedance. Also, the substrate and the permittivity are changed, contributing to the enhancement of the bandwidth and other parameters [14].

This chapter will give you insights into how the slotted patch is used to increase the bandwidth of the antenna.

4.1. Choosing a Design Method

We did a literature study on how to increase the performance of the antenna and we ended up finding two design methods. One method is to use a

passive resonator on top of the patch, and another is to use slots in the patch. The design model is shown in the figures below,
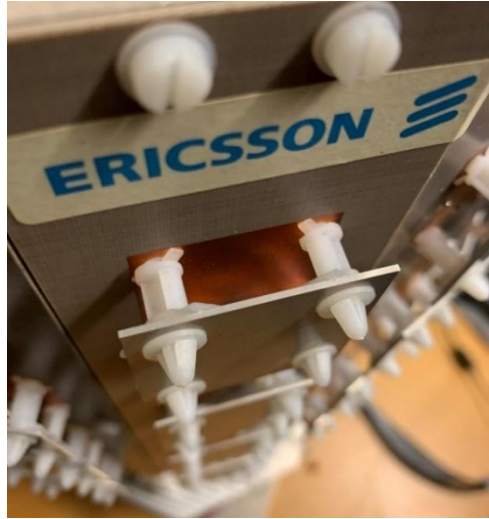
Figure 4.1: Example of passive resonator placed on top of the patch.
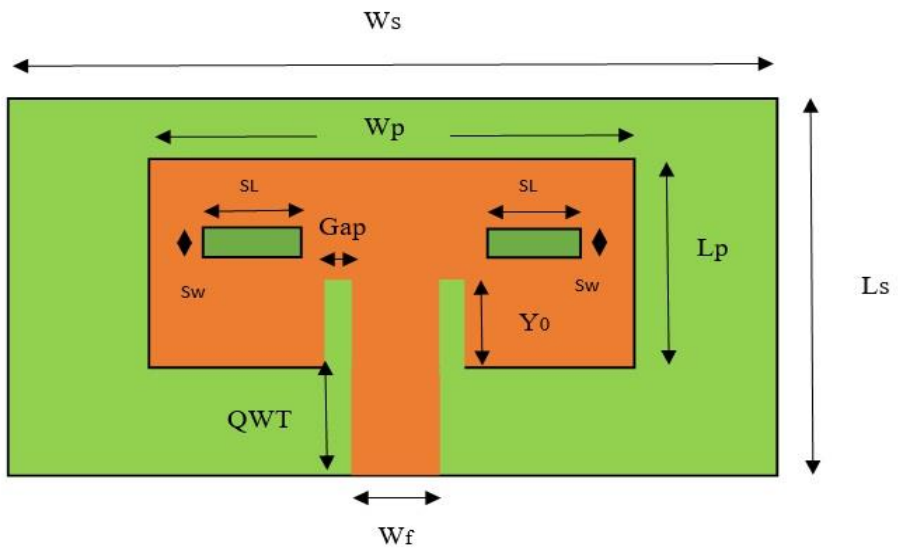
Figure 4.2: Design of Slotted patch.

where

- Ws = Width of the substrate
- Ls = Length of the substrate
- Wp = Width of the patch
- Lp = Length of the patch
- Yo = Inset depth
- Gap = Inset gap or width
- QWT = Quarter wavelength transformer
- W_f = Width of the feed
- SL = Slot length
- Sw = Slot width

Initially, we experimented with both design methods to enhance the performance of the antenna. On multiple trials, we got a poor reflection coefficient at the resonant frequency with the passive resonator design and thereby took a long time to redesign the antenna to achieve the result. Meanwhile, we started getting better results in the slotted patch design than from the passive resonator design. After working further with the slotted patch, we achieved the expected results for our project. So, we chose a slotted patch design. The following section examines the effects of the slots in the patch on the antenna performance.

4.2. Design of Slotted Patch

The design procedure for a slotted patch is the same as we did for the antenna without slots. However, there is a major difference in the permittivity and the substrate used. The substrate also contributes to the performance of the antenna. The thicker it is, the larger the bandwidth, and it also contributes to an increase in the gain. Since we aim for a higher gain, we chose a substrate with low loss, we increased the size of the ground plane, and we chose an appropriate feeding method. So, for this design, we have chosen RT/duroid 5880 substrate with permittivity equal to 2.2 [15].

The effects of the slots on the antenna performance are shown below.

4.2.1. Effect of Slot Length

In Table 4.1, you can see that the change in the slot length affects the reflection coefficient and the resonant frequency. When the length is increased the resonant frequency drops consistently, but the reflection coefficient decreases drastically initial but then stabilizes to a higher value. The values of the slot length are randomly selected to study how the resonant frequency and reflection coefficient are influenced. The obtained resonant frequency in the table was found using the measure tool on the plot for more accuracy.

Slot Length(mm)	Resonant Frequency (GHz)	Reflection Coefficient (dB)
0.5	5.84	-31.1
1.0	5.80	-45.1
1.5	5.77	-36.6
1.8	5.74	-35.6

Table.4.1: Effect of the slot length on resonant frequency and reflection coefficient.
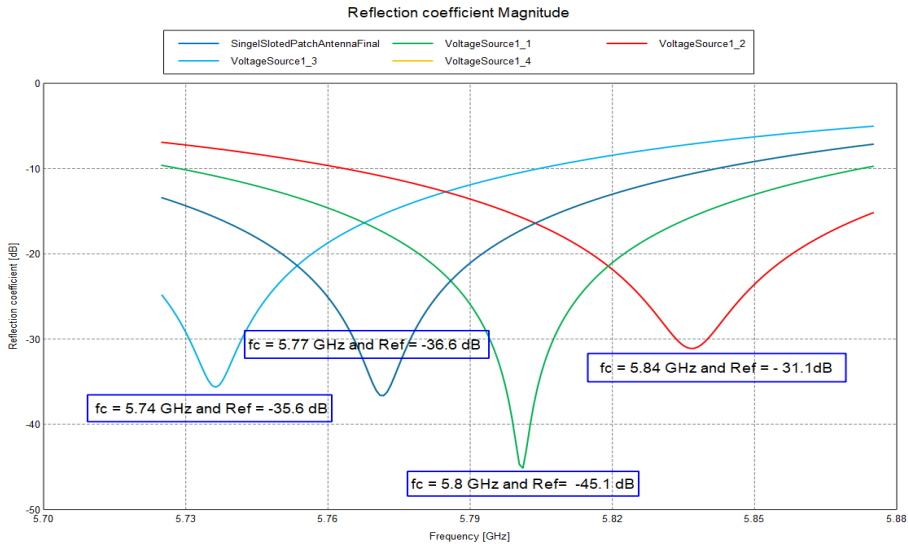
Figure 4.3: Effect of the slot length on reflection coefficient (dB). Refer to Table 4.1 to relate each curve to a slot length.

4.2.2. Effect of Slot Width

The width of the slot influences the resonant frequency and the reflection coefficient. When the width is increased then there is a drop in the resonant frequency and there is a decrease in the reflection coefficient. However, as the slot width is further increased to 5.04mm, the reflection coefficient is increased.

Slot Width(mm)	Resonant Frequency (GHz)	Reflection Coefficient (dB)
4.68	5.82	-35.8
4.74	5.81	-37.56
4.84	5.80	-45.3
4.94	5.784	-50.2
5.04	5.77	-37.2

Table.4.2: Effect of the slot width on resonant frequency and reflection coefficient.
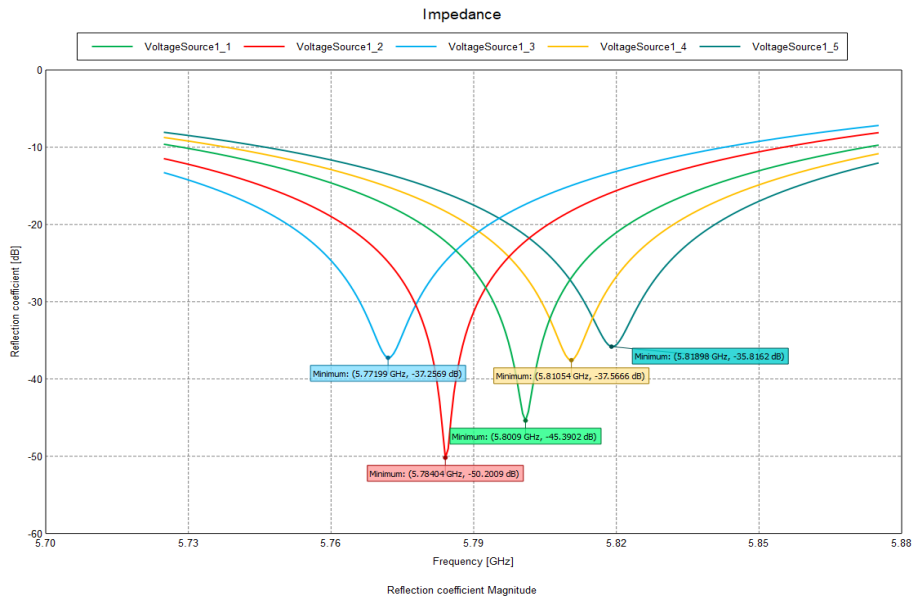
Figure 4.4: Effect of the slot width across reflection coefficient (dB). Refer to Table 4.2 to relate each curve to a slot width.

4.3. Theoretical and Simulated Values for the Slotted Patch Antenna

4.3.1. Transmitter Antenna

The theoretical calculations are done using the formulas in the previous chapter for the slotted patch and the values are shown in Table 4.3 below. However, there is no calculation for the slot used in the patch. So, we used a random value for both the length and width of the slot.

As we saw in the previous chapter (Section 3.3), there will be differences between the theoretical values to the simulated. The parameters obtained from the formulas are just an approximation of how the design can look. However, we redesign the antenna by tuning a few parameters during simulation to get the results needed. The exact values from the simulations for the transmitter antenna are shown in Table 4.4.

Parameters	Values (mm)
Length of the patch	15.016
Width of the patch	20.446
Inset depth	5.147
Inset width	0.5
Length of quarter wavelength transformer	4.725
Width of quarter wavelength transformer	2.75
Length of the slot	1
Width of the slot	3

Table 4.3: Parameters from theoretical calculations for transmitter antenna.

Parameters	Values (mm)
Length of the patch	15.0857
Width of the patch	20.4458
Inset depth	4.2746
Inset width	0.5
Length of quarter wavelength transformer	6.464
Width of quarter wavelength	2.67

transformer	
Length of the slot	1.02
Width of the slot	4.82

Table 4.4: Parameters from simulations for transmitter antenna.

4.3.2. Receiver Antenna

In the same way, the results from the theoretical formulas and simulations for the receiver antenna are shown in Tables 4.5 and 4.6.

Parameters	Values (mm)
Length of the patch	6.513
Width of the patch	10.223
Inset depth	2.186
Inset width	0.5
Length of quarter wavelength transformer	4.725
Width of quarter wavelength transformer	2.575
Length of the slot	1
Width of the slot	2

Table 4.5: Parameters from theoretical calculations for receiver antenna.

Parameters	Values (mm)
Length of the patch	7.239
Width of the patch	8.472
Inset depth	0.488
Inset width	0.5
Length of quarter wavelength transformer	2.717
Width of quarter wavelength transformer	1.08
Length of the slot	1
Width of the slot	2.55

Table 4.6: Parameters from simulations for receiver antenna.

4.4. Simulation Results

The plots from the simulations of antenna gain, VSWR, reflection coefficient, and impedance for both the transmitter and receiver antennas are given below. The maximum gain is obtained from the polar plot.

4.4.1. Transmitter Antenna
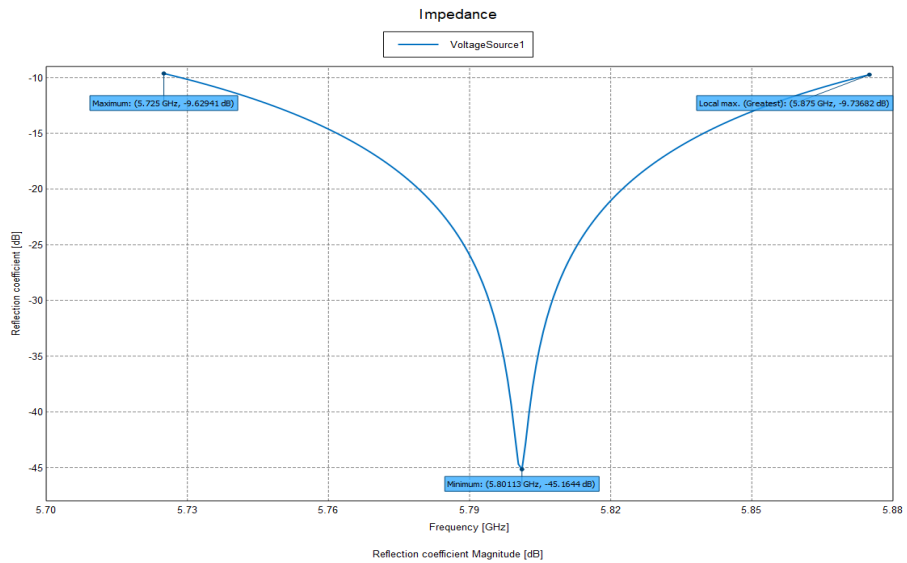
Figure 4.5: Reflection coefficient of slotted patch with -45.16dB at 5.8GHz resonant frequency.
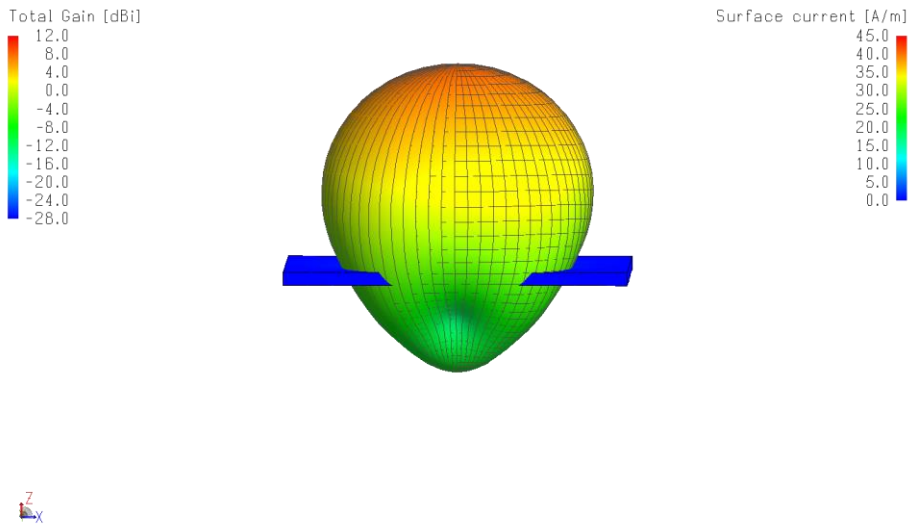
Figure 4.6: 3D gain pattern with maximum gain of 8dBi at 5.8GHz resonant frequency.
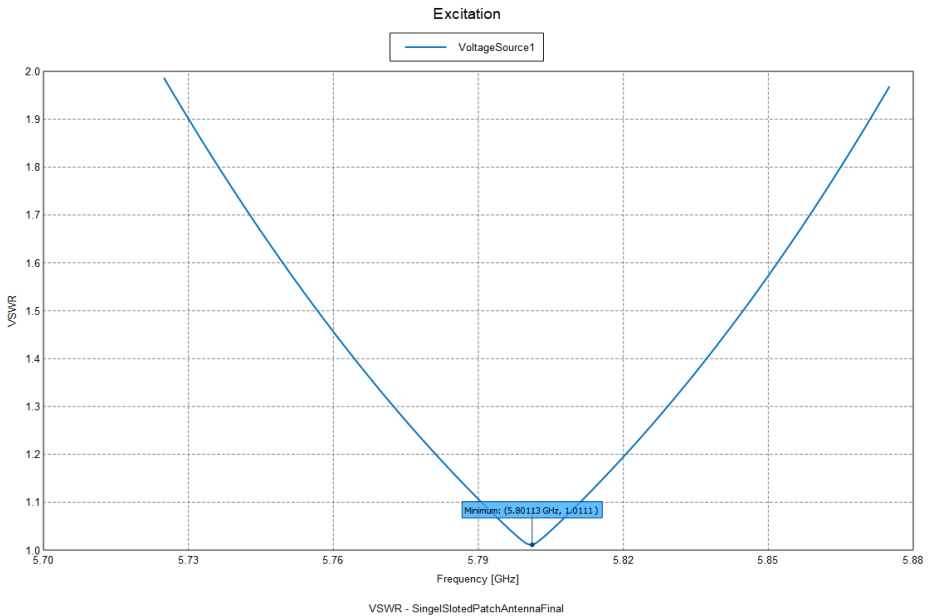
Figure 4.7: VSWR of slotted patch with 1.01 at 5.8GHz resonant frequency.
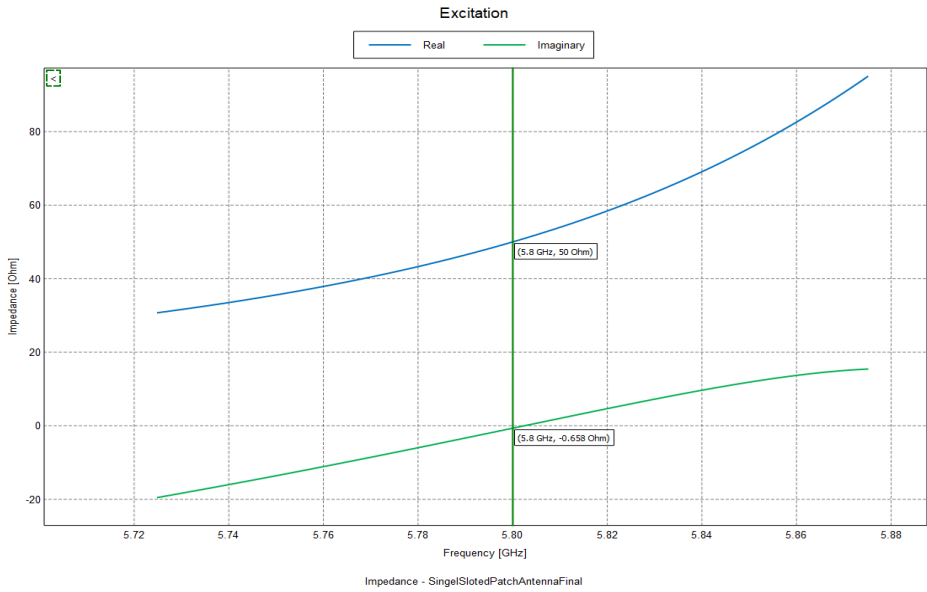
Figure 4.8: Impedance of slotted patch with 50Ω in real part and -0.658Ω in imaginary part at 5.8GHz.
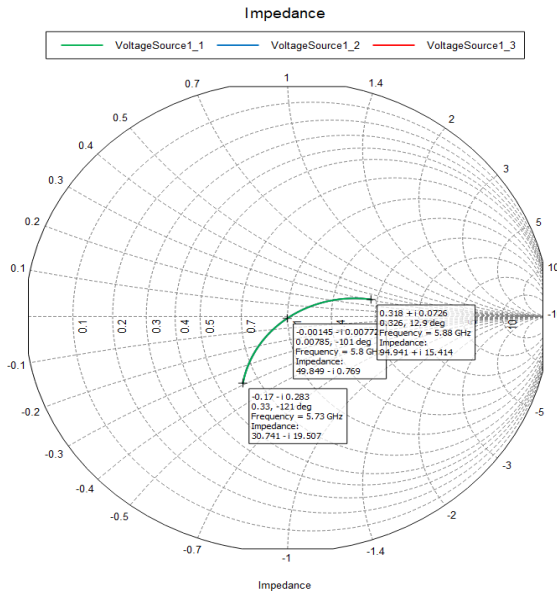
Figure 4.9: Smith chart showing impedance trace in frequency range 5.73-5.88GHz.
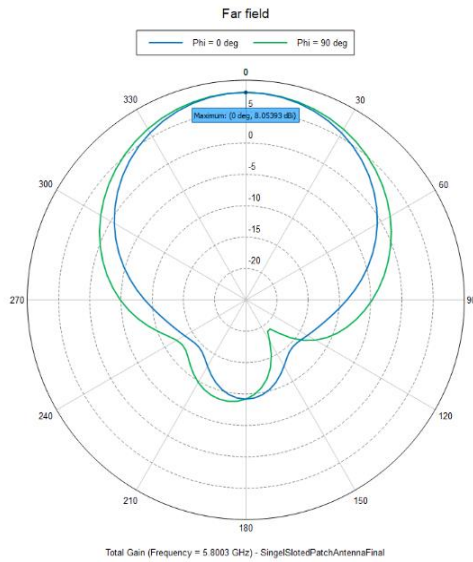
Figure 4.10: Polar plot showing the far field total gain at resonant frequency 5.8GHz in Z plane.

4.4.2. Receiver Antenna
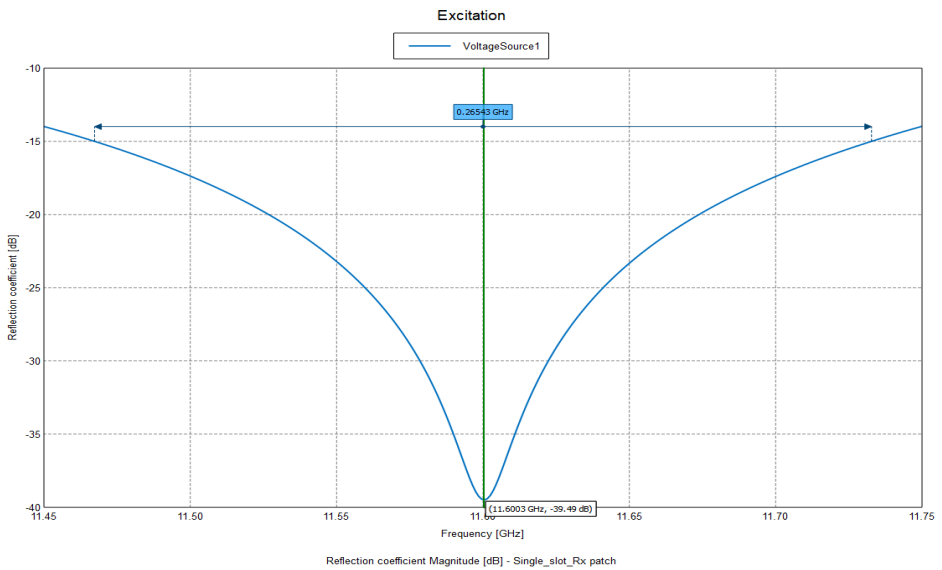
Figure.4.11: Reflection coefficient of slotted patch with -39.49dB at 11.6GHz resonant frequency.
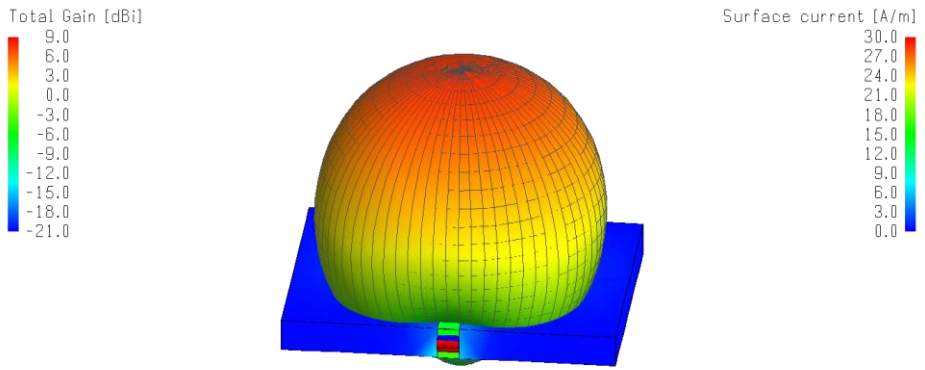
Figure.4.12: 3D gain pattern with maximum gain of 7.6dBi at 11.6GHz resonant frequency.
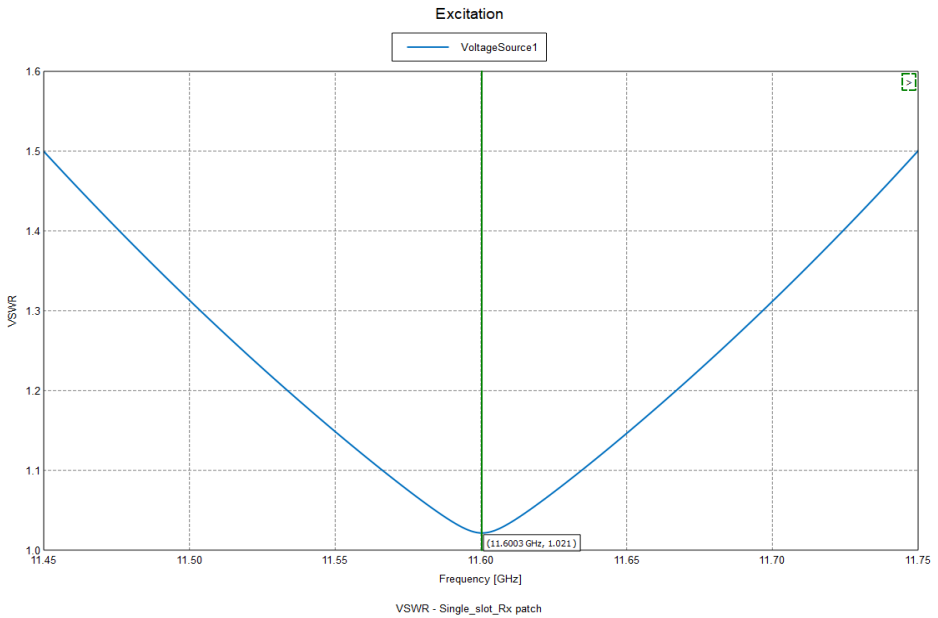
Figure 4.13: VSWR of slotted patch with 1.02 at 11.6GHz resonant frequency.
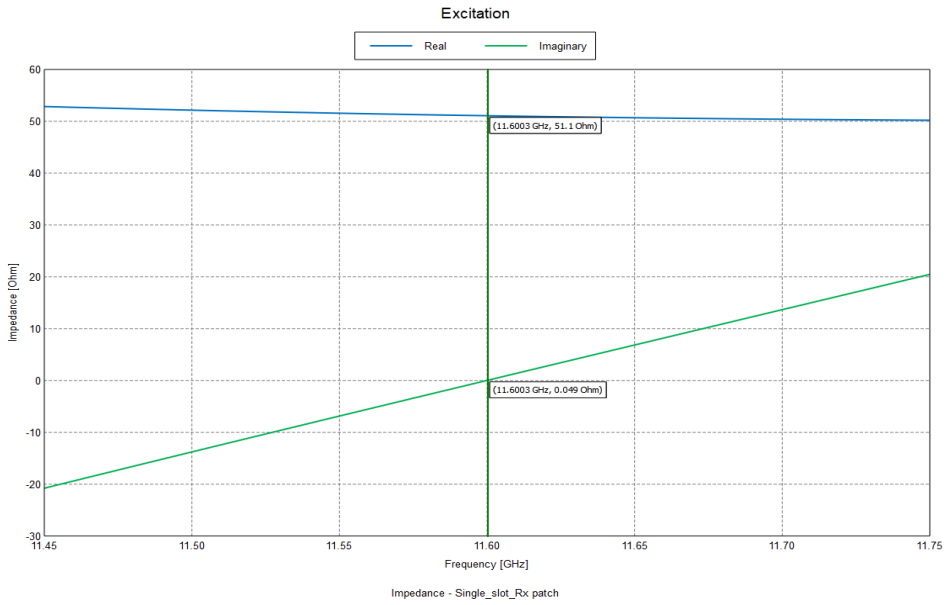
Figure 4.14: Impedance of slotted patch with 51.1Ω in real part and 0.049Ω in imaginary part at 11.6GHz.
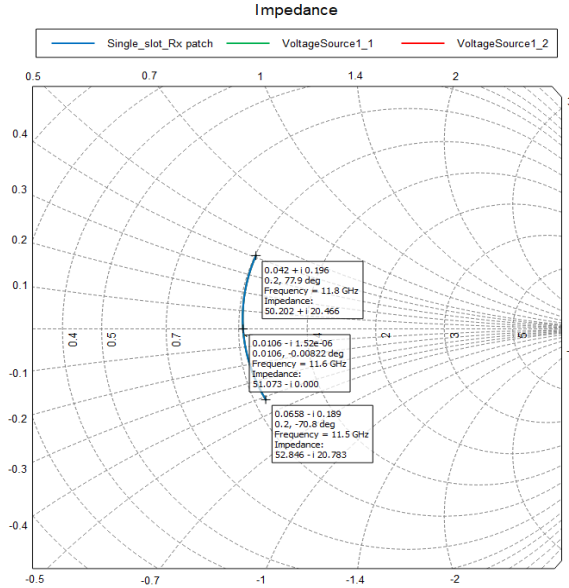
Figure 4.15: Illustration of zoomed in Smith chart showing the impedance trace in the frequency range 11.5-11.8GHz.
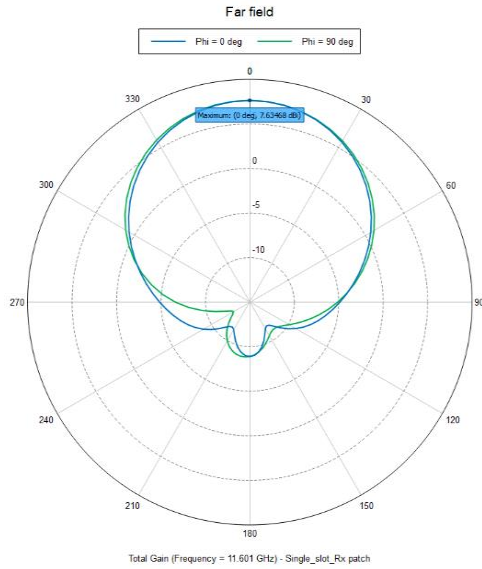
Figure 4.16: Polar plot showing the far field total gain at resonant
frequency 11.6GHz in Z plane.

4.5. Bandwidth Calculation

"Bandwidth of an antenna refers to the range of frequencies over which an
antenna can operate efficiently" [16]. Certain parameters like radiation
pattern, gain and VSWR may need to satisfy some performance requirement
within the bandwidth.

Generally, the bandwidth is calculated using the VSWR parameter which is
called the impedance bandwidth. The commonly used VSWR specification
is 2:1, which means the range of frequency that is below VSWR = 2 is
chosen as operating bandwidth [16].

We can also specify the bandwidth as percentage bandwidth using the
formula below. We need to use the center frequency of operation, which in
our case is 5.8GHz for the transmitter antenna and 11.6GHz for the receiver
antenna:

$$BW = 100 \times \frac{F_H - F_L}{F_C}$$

(4.1)

F_H = Highest frequency in the band

F_L = Lowest frequency in the band
F_C = Center frequency in the band

In our thesis, we represent the bandwidth using the formula below [6]:

$$BW = f_2 - f_1 \hspace{5cm} \textbf{(4.2)}$$
f_1 = Lowest frequency in the band
f_2 = Highest frequency in the band

4.5.1. Transmitter Antenna without Slot

Since f_1 = 5.779GHz, f_2 = 5.8242GHz
From (4.2), $BW = f_2 - f_1$ = 5.8242 – 5.779 = 0.0452GHz = 45.2MHz

4.5.2. Transmitter Antenna with Slot

Since f_1 = 5.7567GHz, f_2 = 5.8448GHz
From (4.2), $BW = f_2 - f_1$ = 5.8448 – 5.7567 = 0.0881GHz = 88.1MHz

4.5.3. Receiver Antenna without Slot

Similarly,
since f_1 = 11.5018 GHz, f_2 = 11.6982 GHz
BW = 11.6982 – 11.5018 = 0.1964GHz = 196.4MHz

4.5.4. Receiver Antenna with Slot

Since f_1 = 11.45GHz, f_2 = 11.7496GHz
BW=11.7496 – 11.45 = 0.2996GHz = 299.6MHz

4.6. Comparison of Results

We have compared the results from both designs (with and without slot) in the table below for a better understanding.

4.6.1. Comparing Transmitter Antenna

Parameters	Without Slot	With Slot
Gain (dBi)	6.9	8
VSWR	1.02	1.01
Reflection Coefficient (dB)	-39.85	-45.16
Impedance (Ω)	49.3	50
Bandwidth (MHz)	45.2	88.1

Table 4.7: Comparison of transmitter antenna results with slot and without slot.

4.6.2. Comparing Receiver Antenna

Parameters	Without Slot	With Slot
Gain (dBi)	6.9	7.6
VSWR	1.01	1.02
Reflection Coefficient (dB)	-46.2	-39.49
Impedance (Ω)	49.9	51.1
Bandwidth (MHz)	196.4	299.6

Table 4.8: Comparison of receiver antenna results with slot and without slot.

From the above Tables 4.7 and 4.8, we can see that the bandwidth has been enhanced drastically using the slotted patch than the patch antenna without a slot. This is due to various parameter changes discussed in Section 4.2. Thus, the slotted patch is used further in our project to attain the requirements for the proposed radar system.

Chapter 5

Design of Transmitter Antenna array

This chapter will give you the details on how an antenna array is designed. "Antenna array is a set of multiple antenna elements connected which works as a single antenna to transmit or receive the radio waves" [17]. These antenna elements are combined with a feeding line through which all the elements are connected as one antenna. The radio waves from each element contribute to a constructive interference to increase the power radiated in a certain direction.

An antenna array can be used to increase the gain of the antenna beyond that from a single antenna element. In general, the larger the number of antenna elements, the higher the gain. This increase in gain thereby will result in a narrow beam. We expect to have a 20dBi gain at the transmitter antenna and a 26dBi gain at the receiver antenna. So, we designed two antenna arrays to satisfy our requirements, one each for the transmitter and receiver.

5.1. Types of Array Designs

Initially, we started designing an antenna array with two antenna elements, then with four antenna elements, a 2+4 array, and finally, we designed a 2×4 transmitter array antenna [11]. The different array designs are shown in the figure below,
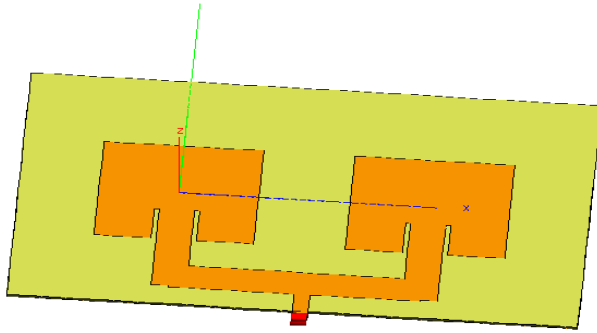
Figure 5.1: Design of array with two antenna elements.
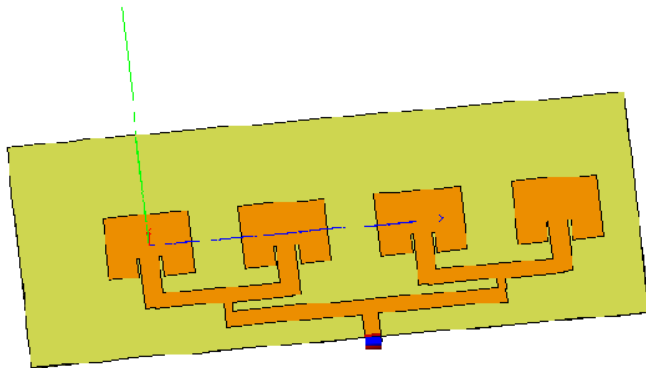
Figure 5.2: Design of array with four antenna elements.
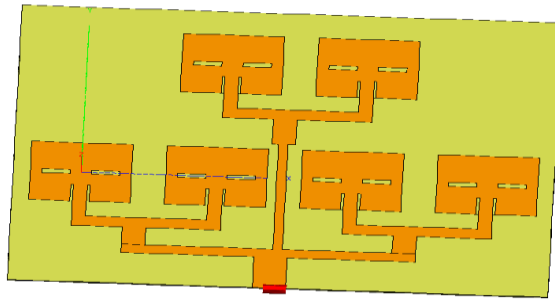
Figure 5.3: Design of array with 2+4 antenna array.
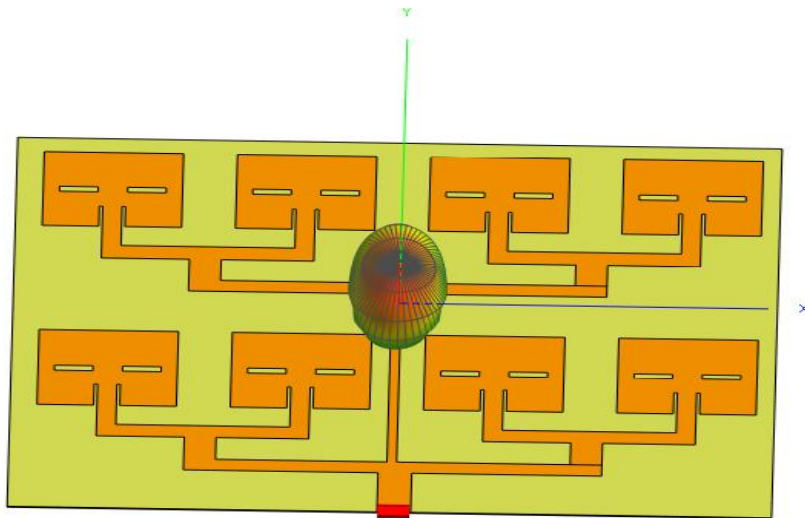
Figure 5.4: Final design of 2×4 transmitter antenna array at 5.8GHz.

5.2. Impedance Matching Technique

An important task while designing an antenna array is to choose the best power divider to be placed in between the antenna elements. There are different power dividers like the Gysel power divider, and the simplest power divider is accomplished by using quarter-wave transformer with 70.71Ω to match 100Ω to 50Ω transmission line [18]. By using a quarter wavelength transformer, we get better return loss, larger -10dB bandwidth, and efficiency with good beamwidth.

The basic things to keep in mind while designing a power divider are an equal division of power between elements, good amplitude, phase balance, and impedance matching. Once the impedance matching is done, we find the dimensions of the quarter wavelength transformer. In our case, we used the quarter wavelength with permittivity to achieve the necessary dimension for the power divider [19]. The formula is shown below:

$$L_q = \frac{\lambda}{4\sqrt{\varepsilon_r}} \tag{5.1}$$

The design of the antenna with quarter-wavelength transformer is shown in Fig. 5.5. We have used a single-section quarter wavelength transformer. The working principle is such that we feed 50Ω impedance at the quarter wavelength transformer which has a characteristic impedance of 70Ω. This 50Ω is split in between the line connecting the left and right antenna elements having characteristics impedance of 100Ω with 50Ω on either side. This transmission line with a characteristic impedance of 70Ω converts 50Ω to 100Ω to be able to have an equal split. The characteristic impedance of the quarter wavelength transformer is found using the formula in (5.2). The illustration of the above text is shown below in Fig. 5.5.

Using the formula 5.2 we can find the characteristic impedance of the quarter wavelength transformer.

$$Z_C = \sqrt{Z_0 Z_L} \tag{5.2}$$
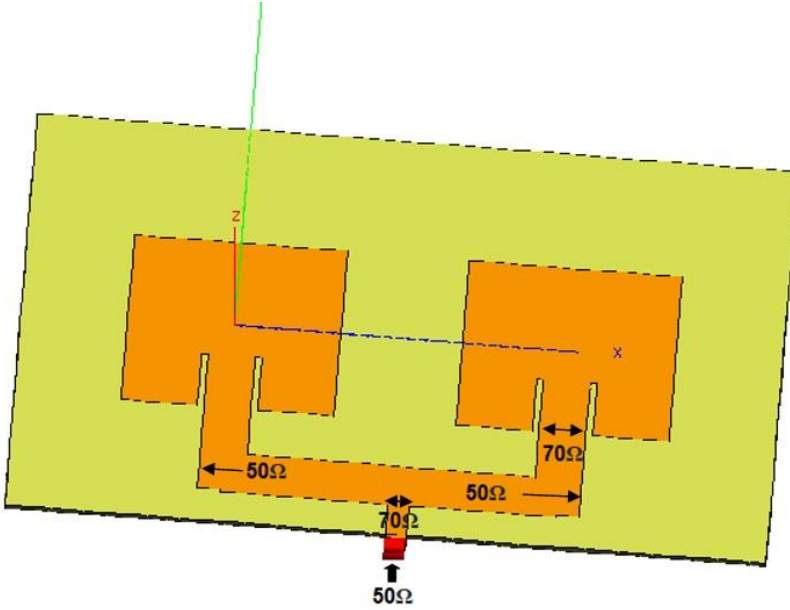
Figure 5.5. Illustration of the impedance split for two antenna elements.

Having found the characteristic impedance of the quarter wavelength transformer, formula (5.3) is used to find the width of the quarter wavelength transformer matching with 50Ω impedance. This technique is followed for every array connector to match the impedance with the antenna array.

$$Z_C = \begin{cases} \dfrac{60}{\sqrt{\varepsilon_{reff}}} \; ln\left[\dfrac{8h}{Wf} \; + \dfrac{Wwf}{4h} \; \right] \;, \; \dfrac{Wf}{h} \leq 1 \\ \dfrac{120\pi}{\sqrt{\varepsilon_{reff}\left[\dfrac{Wf}{h}+1.393+0.667 \; ln\left(\dfrac{Wwf}{h}+1.444\right)\right]}} \;, \dfrac{Wf}{h} > 1 \end{cases} \tag{5.3}$$

Firstly, we designed and tested two and four antenna elements in the FEKO software having a two-way split, as shown in Figs. 5.1 and 5.2. However, we did not get the desired result with the two-way split and few antenna elements. So, we then designed an antenna array with six and eight antenna elements as shown in Figs. 5.3 and 5.4 with a three-way split. We did not

51

achieve enough gain from the 2+4 antenna array. So, we designed an antenna array with 2×4 antenna elements as shown in Fig. 5.4. The upper part of the array (i.e., 1×4 array) is already designed and tested in FEKO software as shown in Fig. 5.2. The lower part of the array is the exact copy of the upper array already designed as shown in Fig. 5.4. We used the translate copy tool to exactly copy the design of the upper patch to the lower patch having the same impedance matching. The important task here is again matching the impedance of 50Ω. We know that the characteristic impedance of the transmission line connecting the left and right of the upper/lower antenna elements is 100Ω and thus characteristic impedance of the transmission line connecting the upper /lower array is 83Ω. This transmission line with characteristic impedance of 83Ω converts 100Ω to 50Ω and thus the upper and lower part of the arrays are connected. The illustration for the above text is shown in Fig. 5.6.

Figure 5.6. Illustration of the impedance split for 2×4 antenna array.

For designing the antenna array, we need the dimensions of the array feeder. An array feeder is a power divider that is responsible for the transmission, reflection, and isolation properties. The dividers may have three ports, four ports, or maybe more and can be lossle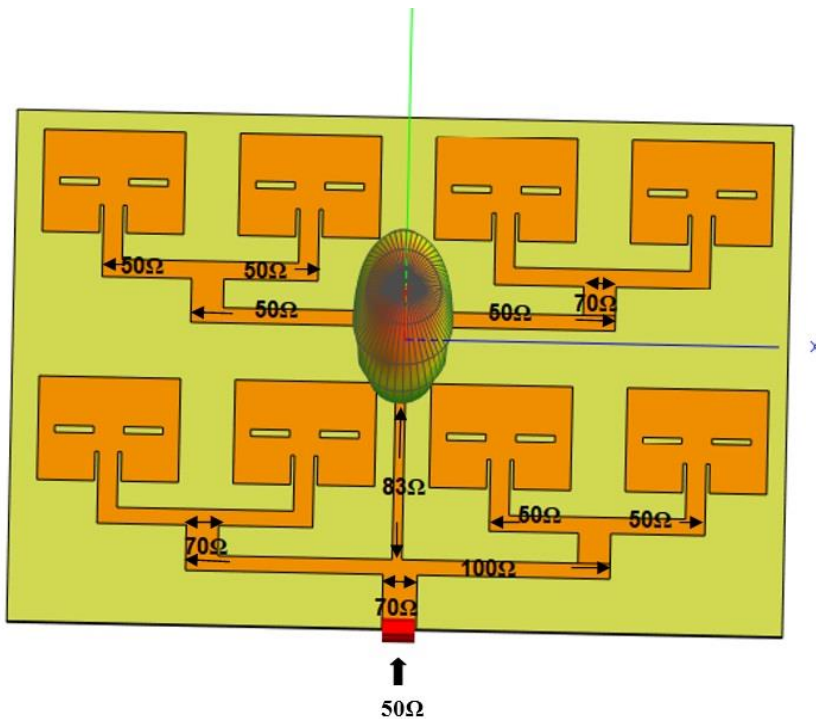ss. The dividers with three ports look like a T-junction while the one with four ports looks like directional couplers and hybrids. Power dividers are used to provide an in-phase output signal with an equal power division ratio (3dB), but an unequal power division ratio is also possible [18].

The distribution of current among the antenna elements depends on the feeding network. A suitable feeding network accumulates all the induced voltages to feed into one point. "A corporate feed network can vary power distribution among antenna elements and can steer the beam by introducing phase change" [20]. Looking at Fig. 5.7, we can see that the current declines at the edge of antenna elements. There is a difference between the upper and lower 1×4 antennas (sub)arrays. The current (and voltage) distribution in the antenna depends upon the type of antenna used. Thus, for a microstrip antenna, the current has a maximum value at the center while the current is zero at the edge and the voltage is out of phase with the current. A half-wavelength away at the start of the patch, the voltage has equal magnitude but is out of phase. The feed points on a resonant center-fed half-wave dipole occur at the point of minimum voltage and maximum current, which enables the most efficient power transfer from the transmitter. This is the basic ideology behind the current distribution in a patch antenna fed at the center.

However, in our case, the antenna array is fed at the bottom and thus most of the current is distributed close to the feed while there is less/no current at the edge of the antenna elements. The difference between the current intensity of the upper and lower subarrays is due to the power divider giving the upper subarray only 1/3 of the current, resulting in half as much current reaching each of the element in the upper subarray compared to those in the lower subarray. During the simulations, we changed a few parameters of the antenna array to obtain the required output. These parameter changes also contribute to the fluctuation in the current distribution in Fig. 5.7.
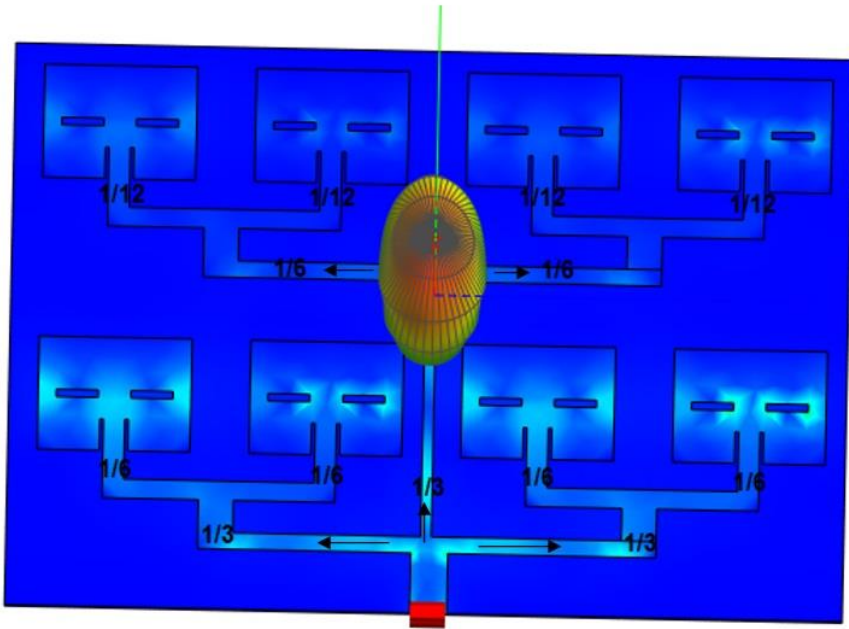
Figure 5.7. Illustration of current distribution for transmitter antenna array.

5.3. Antenna Array Gain

Array gain refers to the amount of power achieved by the transmitter or receiver by using N antenna elements or antennas. The antenna elements can be designed in a 1 or 2-dimensional array. The array factor decides the radiation pattern of the antenna in accordance with the number of elements used.

This factor measures the effect of combining radiating elements in an array without considering individual antenna elements. The overall radiation pattern of an array is determined by the array factor in combination with the radiation pattern of the antenna element. Arrays can be designed either to radiate broadside (i.e., radiation perpendicular to the array orientation) or to radiate end-fire (i.e., radiation in the same direction as the array orientation) [21]. There are other factors influencing the antenna array gain, they are:

- **Number of Antenna Elements: "**Array directivity increases as the number of elements keeps increasing. For all arrays, the spacing between elements is 0.4 times the wavelength. The number of side lobes and the sidelobe level increase with the number of elements. It is important to note that the number of main lobes is determined upon the array factor" [21].

- **Influence of Antenna Element Spacing:** "Array factor is highly influenced by element spacing as well. The higher the element spacing, the higher the directivity. In general, the element spacing is kept smaller than $\lambda/2$ to prevent grating lobes from occurring. Another unwanted peak value in the radiation pattern of an array is a grating lobe. A spacing beyond λ becomes unworkable, resulting in multiple unnecessary grating lobes" [21].

- **Influence of the Radiating Element Properties:** We will consider different cases for a better understanding of the influence of radiating elements.

  - When there is a radiation pattern of an isotropic element, "since an isotropic element radiates the same amount of energy in all directions, the overall radiation pattern is the same as the array factor" [21].

  - When there is a radiation pattern of a dipole, "the overall radiation pattern is clearly different from the array factor, i.e., the directivity has increased with the dipole's directivity and radiation pattern are slightly modified as a result of the dipole's radiation pattern" [21].

  - When there is a radiation pattern of a dipole on an infinite ground plane, "the dipole has a radiation lobe in broadside and thus the directivity of the dipole has increased with 3dB. Also, the overall array does not radiate in directions where the antenna element does not radiate" [21].

Another important factor influencing the array performance is the feed network. The feed depends on the number of elements, amplitude and phase difference between elements, and beam steering. Any modification in the array will influence the performance of the array. When phase distribution is optimized for beam steering then new side lobes will appear, in the same

way the efficiency of the array will decrease when the power is optimized for reducing side lobes [21].

5.4. Directivity and Antenna Array

The directivity of an antenna array is calculated as follows [22]:

$$D_{dir}(dB) = 10\log\left(k \times \frac{4\pi A}{\lambda_0{}^2}\right)$$
(5.4)

 where
A = physical area of the antenna ground,
k (0 ~ 1) = effective coefficient.

For the given value $k = 1$, the theoretical approximation of the maximum directivity is

$$D_{max}(dB) = 10\log\left(\frac{4\pi A}{\lambda_0{}^2}\right)$$
(5.5)

For our antenna array design, the maximum allowed area of the antenna aperture for both transmitter and receiver array are $200 \times 300\text{mm}^2$. For the transmitter antenna, the aperture area for the final design is 75.55×112.12mm. With the center frequency of 5.8GHz, the wavelength is $\lambda_0 = 51.72\text{mm}$. Having all these values substituted in the above formula (5.5), we get a maximum directivity of 15.99 ≈ 16dB. The directivity from the simulation is $D_{dir} = 14.8 ≈ 15$dBi. In the same way, for the receiver antenna, the aperture area from the final design is 55×51.80mm with a center frequency of 11.6GHz, the wavelength is $\lambda_0 = 25.80\text{mm}$. Having all these values substituted in the above formula (5.5), we get a maximum directivity of 17.24dB. The directivity from the simulation is $D_{dir} = 15.7 ≈ 16$dBi.

The aperture efficiency of the antenna is calculated using the formula:

$$k = \frac{\log^{-1}\left(\frac{D_{dir}}{10}\right)}{\log^{-1}\left(\frac{D_{max}}{10}\right)}$$
(5.6)

The aperture efficiency from the above formula is 0.79 for the transmitter array and 0.75 for the receiver array. For a planar array, the aperture

efficiency will be between 0.6 to 0.8. Therefore, the conclusion with directivity and array size is, "if higher directivity is not necessary, the physical area of the antenna can be properly reduced to increase the aperture efficiency. On the other hand, to keep the same physical area of the antenna and increase the number of the array elements, it can be ensured that the antenna has higher directivity with improved aperture efficiency" [22].

5.5. Theoretical and Simulated Values for Antenna Array

The calculations and the formulas are the same as we saw in Chapter 3 for a single patch but there are a few more parameters that must be calculated for the antenna array. Table 5.1 shows you the parameters calculated theoretically.

Parameters	Theoretical Value (mm)	Simulated Value(mm)
Length of the patch	15.0156	15.2257
Width of the patch	20.4458	20.4458
Inset depth	5.1466	4.2326
Inset width	0.5	0.5
Length of quarter wavelength transformer/ sqrt(permittivity)	4.725	6.364
Width of quarter wavelength transformer	2.67	2.84
Length of the slot	1	1
Width of the slot	3	5.65

Table 5.1: Theoretical and simulated values for single antenna element.

As mentioned earlier in Chapter 3, the values obtained with the formula are just approximations of how the antenna can be designed for a given frequency and permittivity. But when comes to the simulation we must change a few parameters to get the expected results. So, the above table gives an outline of the theoretical values and the final values after simulation.

5.6. Simulation Results

The simulation results are plotted below showing the required output for the project. The maximum gain is obtained from the polar plot.
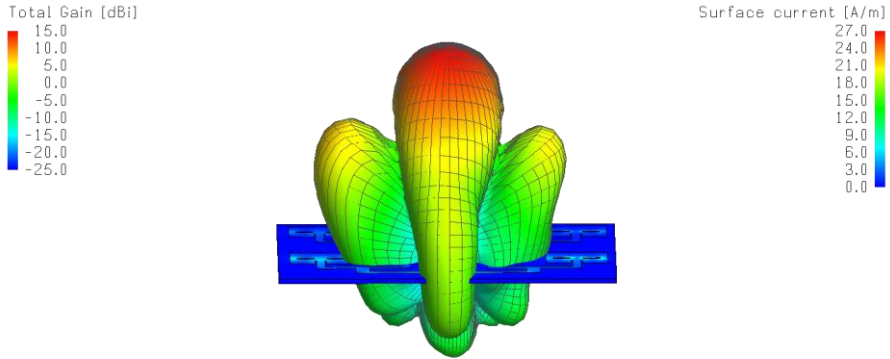
Figure 5.8: 3D gain pattern at resonant frequency of 5.8GHz, with maximum gain of 14.8dBi.
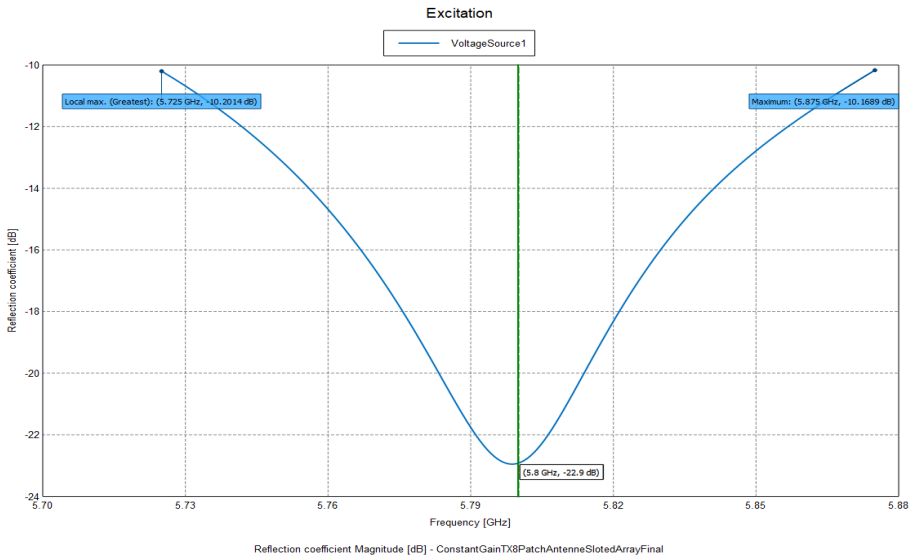
Figure 5.9: Reflection coefficient for transmitter antenna array with -22.9dB at 5.8GHz.
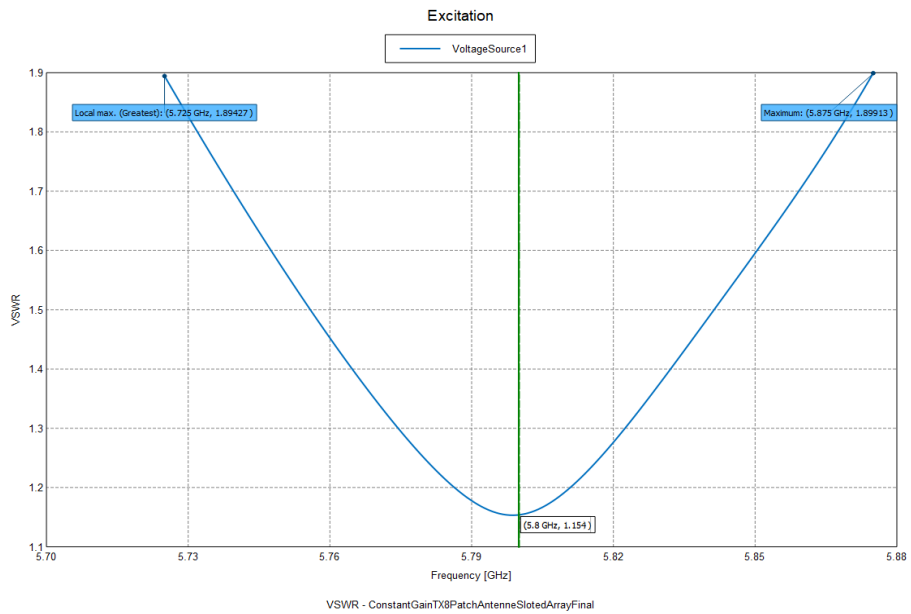
Figure 5.10: VSWR for transmitter antenna array, with 1.154 at 5.8GHz.
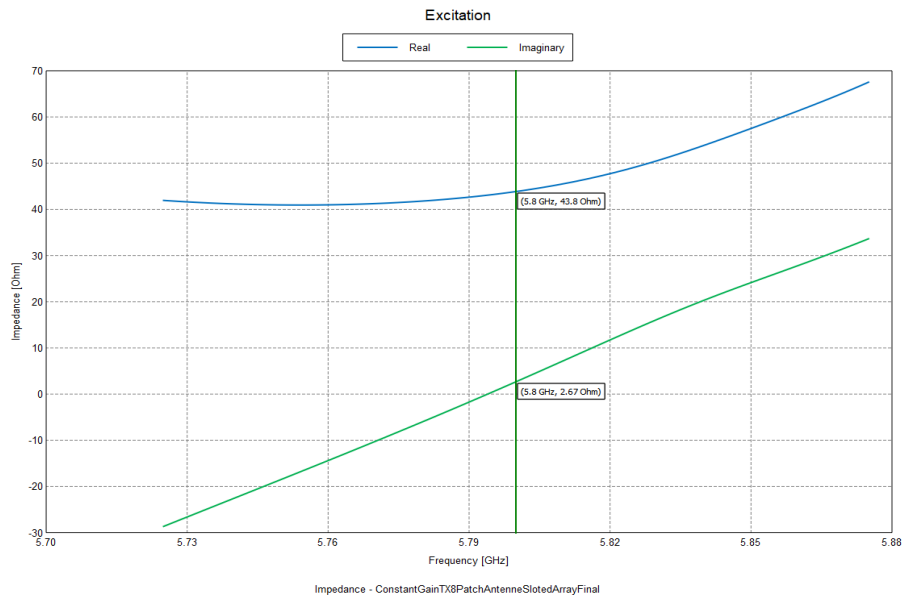
Figure 5.11: Real and imaginary parts of impedance, with 43.8Ω in real part and 2.67Ω in imaginary part at 5.8GHz.

Figure 5.12: Smith chart showing the impedance trace between 5.73-5.88GHz.

Figure 5.13: Polar plot showing the far field total gain at resonant frequency 5.8GHz in Z plane.

60

Chapter 6

Design of Receiver Antenna Array

This chapter will give you details about the antenna array design for the receiver. As we already know we are operating at dual frequencies, i.e., transmitter at 5.8GHz and receiver at 11.6GHz. The challenging part is to neglect the clutters formed in the environment due to propagation mechanisms like reflection, refraction, diffraction, a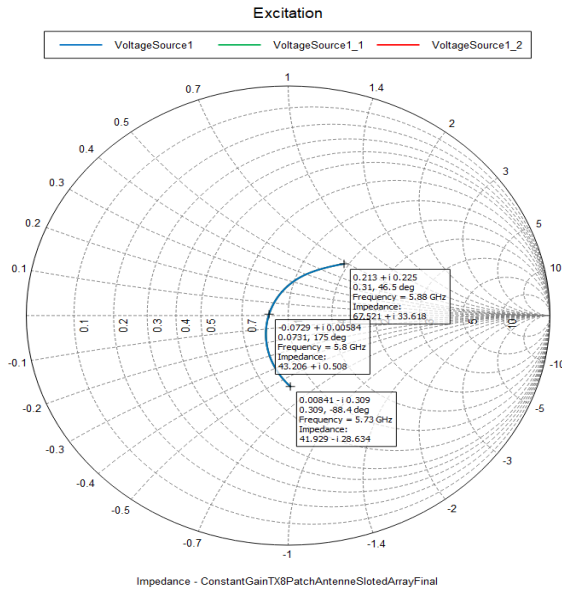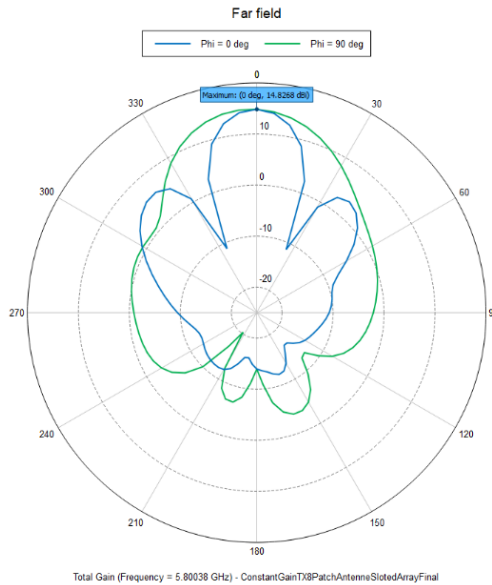nd scattering happening in the channel. To do this we used harmonic radar to operate in second frequency at the receiver. Another challenge is to design the transmitter and receiver array within the given dimension of 200×300 mm. Thus, the coupling of the antenna plays a major role when two antennas are placed close to each other operating at dual frequencies.

6.1. Receiver Antenna Design

The array design for the receiver also followed the same steps as the transmitter array design, but at a different operating frequency of 11.6GHz. Firstly, we designed a 2×6 antenna array as shown in Fig. 6.1 having the transmitter antenna array as a reference. We added four more antenna elements to the right of the antenna array. Two antenna elements at the top and two at the bottom. Then we connected these antenna elements with the already existing 2×4 antenna array using a transmission line. We used the translate copy tool to copy the antenna elements and paste it to the right. Then we matched the impedance to 50Ω which is of importance. Thus, after impedance matching is done following the steps from Chapter 5, we saw unexpected results. The current flow was not equally distributed throughout the patch, thus affecting the gain, reflection coefficient, VSWR, and impedance of the antenna. Also, we found that it would be difficult to

manufacture, and we might face practical difficulties in the manufacturing due to the non-symmetric design of the antenna array. So, we decided to come up with a new antenna array design.

Finally, we designed a 3×4 antenna array for the receiver. We already have a 2×4 antenna array from previously, to which we tried adding another array at the top, as shown in Fig. 6.2. The upper array is the exact copy of the lower array already designed in Fig. 6.4. We used the translate copy tool to exactly copy the design of the lower array to the upper array having the same impedance matching. The steps followed to design the antenna array were the same for both transmitter and receiver except that the dimensions like length, width, and all other structural details will vary according to the operating frequency. The important task here is to match the impedance to 50Ω. We know that the characteristic impedance of the transmission line connecting the left and right of the upper/lower antenna elements is 100Ω and the transmission line connecting upper and lower array is 83Ω. This transmission line with characteristic impedance of 83Ω converts 100Ω to 50Ω and thus the upper and lower part of the arrays were connected.

The characteristic impedance of the quarter wavelength transformer is found using the formula (5.1). Then, the formula (5.2) is used to find the width of the quarter wavelength transformer matching with 50Ω impedance. This technique is followed for every array connector to match the impedance with the antenna array. An illustration of the impedance split is shown in Fig. 6.3.
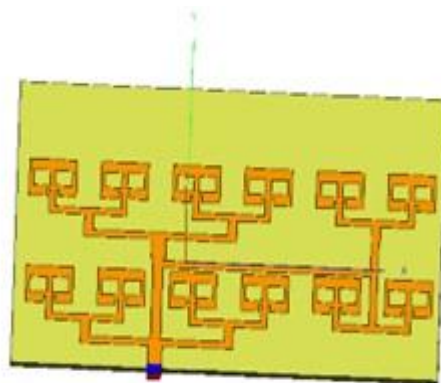

Figure 6.1: Trial work of 2×6 array for receiver.
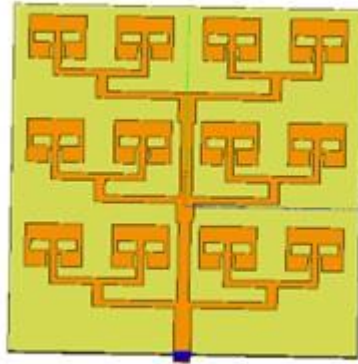
Figure 6.2: Final design of 3×4 array for receiver.
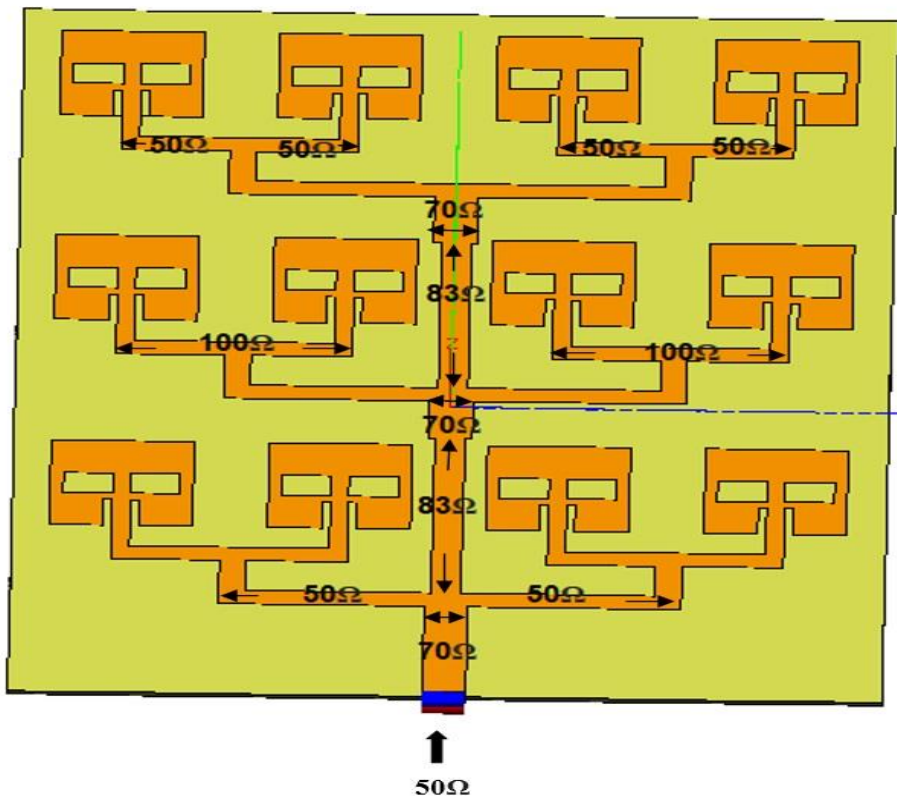
Figure 6.3. Illustration of the impedance split for 3×4 antenna array.

In our design, the receiver antenna array is fed at the bottom and thus most of the current is distributed close to the feed while there is less/no current at the edge of the antenna elements. This is because we gave equal power distribution for all the antenna elements in the array, i.e., the lower antenna array is split into three parts with 1/3 of the current distribution while the one above is split into 1/9 each. The topmost array has a two-way split such that each has a distribution of 1/18. During simulation, we changed a few parameters of the antenna array to obtain the required output. These parameter changes also contribute to the fluctuation in the current distribution. An illustration of how the current is distributed in the antenna array is shown in Fig. 6.4.

Figure 6.4. Illustration of current distribution for receiver antenna array.

6.2. Theoretical and Simulated Values for Antenna Array

The calculations and the formulas are the same as we saw in Chapter 2 for a single patch but there are a few more parameters that must be calculated for the antenna array. Table 6.1 shows you the parameters calculated theoretically.
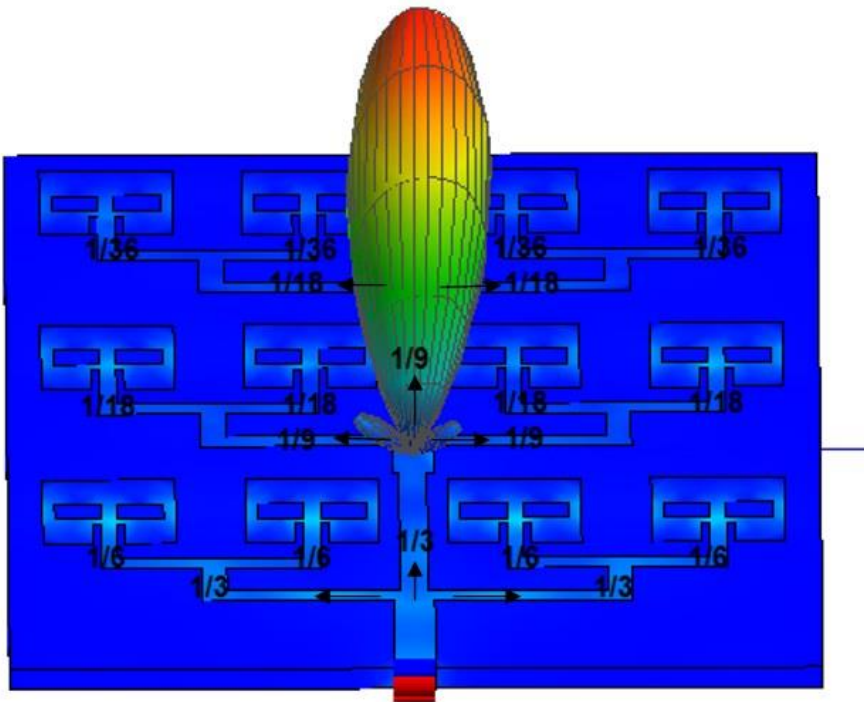
Parameters	Theoretical Value(mm)	Simulated Value(mm)
Length of the patch	6.5135	6.8838
Width of the patch	10.2229	8.4716
Inset depth	2.1859	2.0878
Inset width	0.5	0.5
Length of quarter wavelength transformer/sqrt(permittivity)	4.725	2.717
Width of quarter wavelength transformer	2.575	1.08
Length of the slot	1	1.5
Width of the slot	3	3.035

Table 6.1: Theoretical and simulated values for single antenna element.

As mentioned earlier in Chapter 3, the values obtained with the formula are just approximations of how the antenna can be designed for a given frequency and permittivity. But when comes to the simulation we must change a few parameters to get the expected results. So, the above table gives an outline of the theoretical values and the final values after simulation.

6.3. Simulation Results

The simulation results are plotted below showing the required output for the project. The maximum gain is obtained from the polar plot.
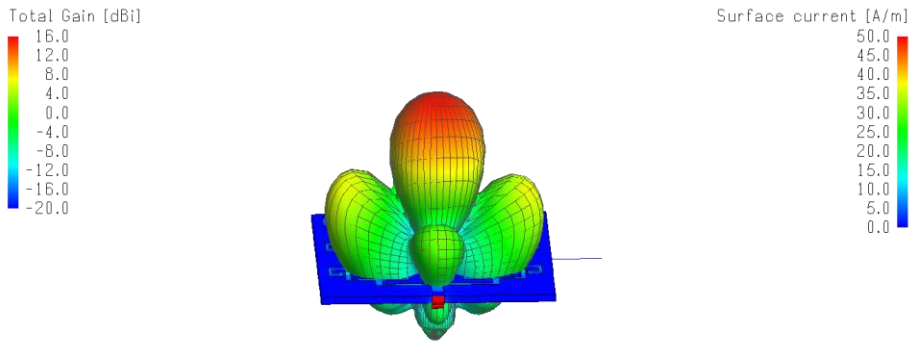
Figure 6.5: 3D gain pattern at resonant frequency of 11.6GHz, with maximum gain of 15.7dBi.
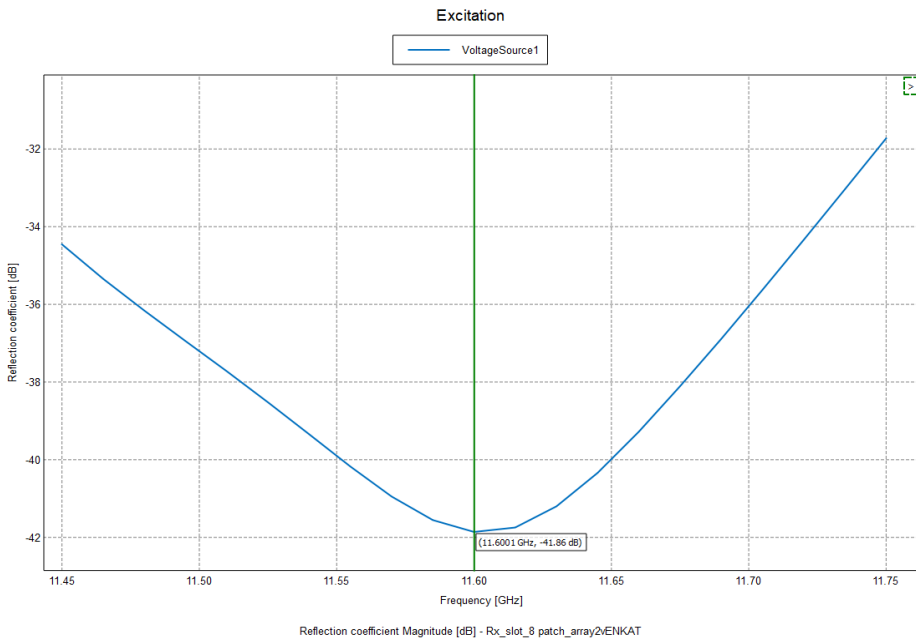
Figure 6.6: Reflection coefficient for receiver antenna array, with -41.86dB at 11.6GHz.
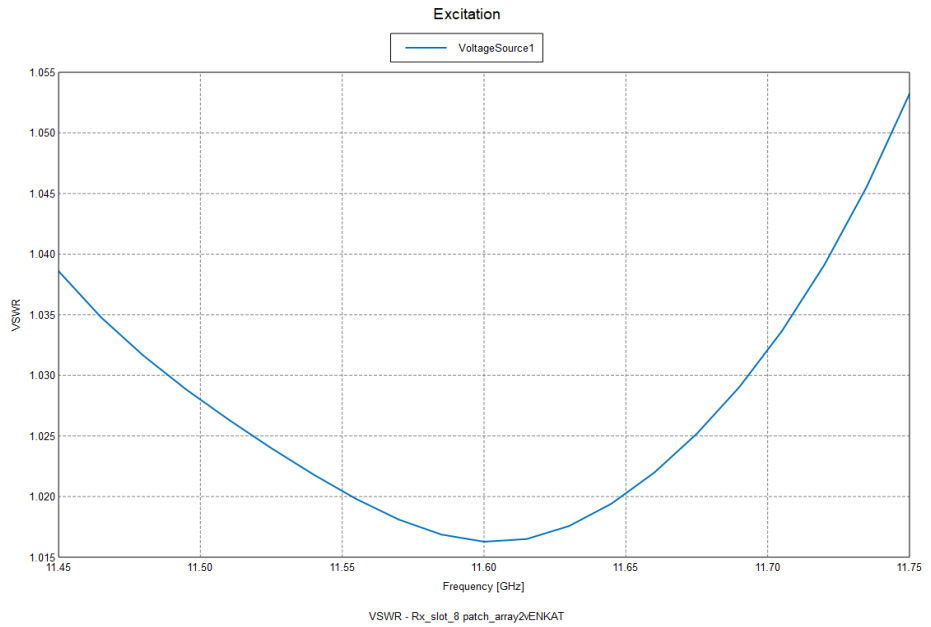
Figure 6.7: VSWR for receiver antenna array, with 1.017 at 11.6GHz.
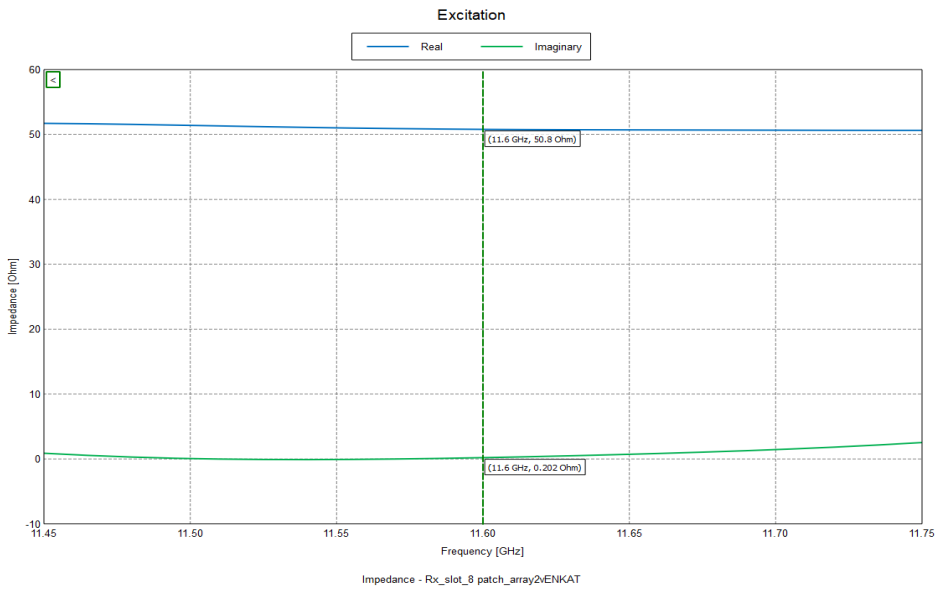
Figure 6.8: Real and imaginary parts of impedance, with 50.8Ω in real part and 0.202Ω in imaginary part at 11.6GHz.
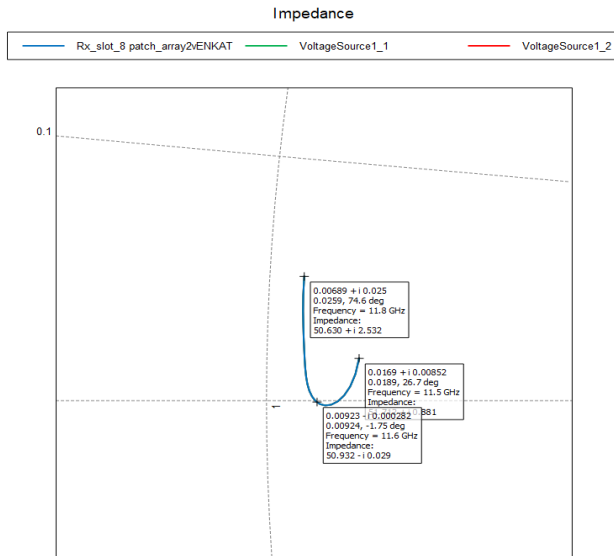
Figure 6.9: Illustration of zoomed in Smith chart showing the impedance trace in the frequency range 11.5- 11.8GHz.
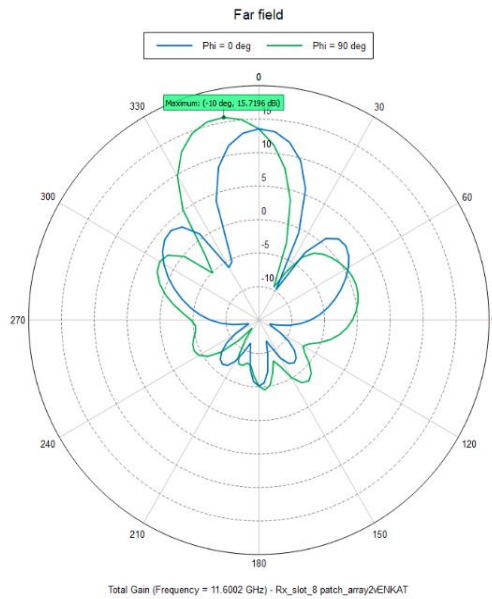
Figure 6.10: Polar plot showing the far field total gain at resonant frequency 11.6GHz in Z plane.

Chapter 7

Manufacturing and Testing

Following the detailed design in the simulation software FEKO, the antenna arrays were manufactured in a research laboratory at the Department of Electrical and Information Technology at Lund University. We ordered the substrates from Rogers Corporation with the same properties and then the antenna arrays were manufactured with the help of Andreas J. Johansson at the research laboratory. The manufactured antenna arrays are shown in Figs.7.1 and 7.2.
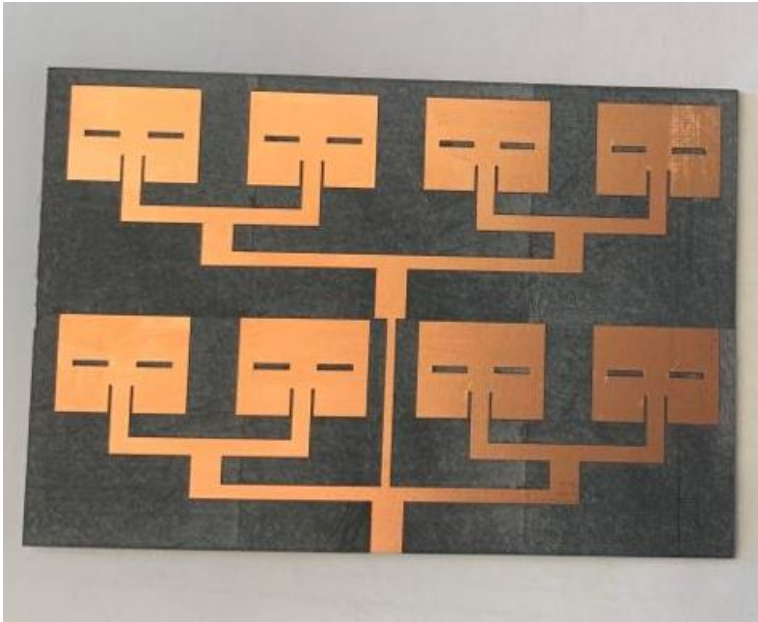
Figure 7.1: Manufactured transmitter 2×4 antenna array without connector

Figure 7.2: Manufactured receiver 3×4 antenna array without connector.

A vector network analyser was used in the lab to measure the reflection coefficient of the 2×4 transmitter antenna array and the result is shown in Fig. 7.3.
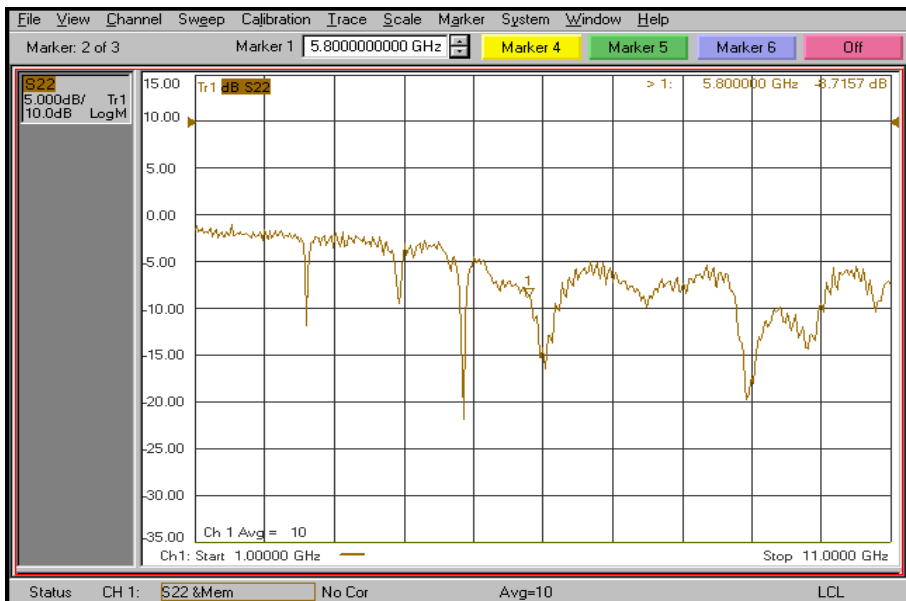
Figure 7.3: Reflection coefficient measured at 5.8GHz using a vector network analyser.

In Fig. 7.3, it can be seen that there is a dip at 6GHz, even though the expected center frequency is 5.8GHz. The reason can be due to the change in the properties of the connector used for the power source. We used an in-built edge port connector when designing the antenna array in the FEKO software. However, it is quite challenging to choose the type of SMA (Sub Miniature version A) connector to relate to the antenna array. Fig. 7.4 shows the kinds of SMA connectors generally used in our testing lab at Lund University. The performance of the antenna can be affected due to different properties of the connector used. This happens in most of the situations due to the geometry of the connector. The properties can be anything like the type of the material used, working voltage of the connector, center and outer contact resistance, insulation resistance, insertion loss, durability, etc.
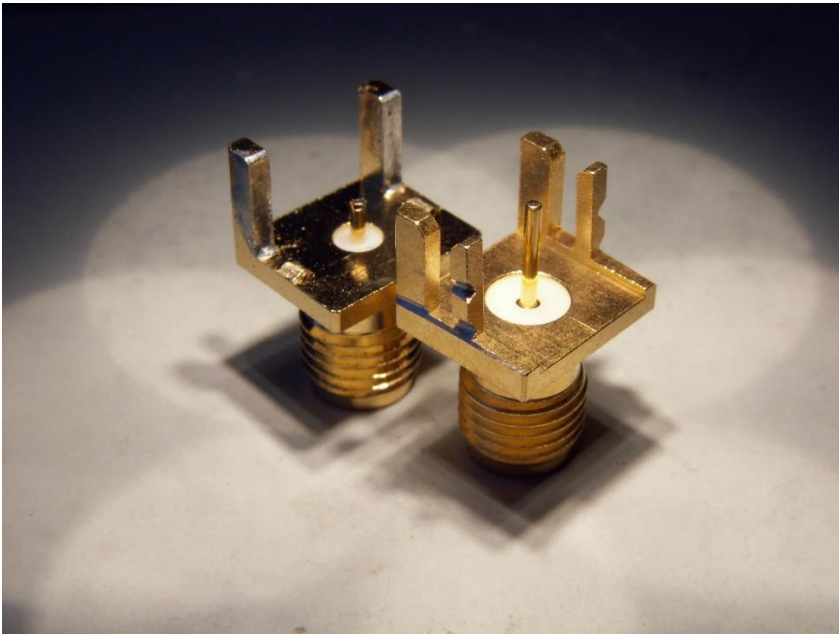
Figure 7.4: Two kinds of SMA connectors for PCB edge mounting.

Of these SMA connectors shown in Fig. 7.4, the connector with the widest outer conductor of 4mm is mounted on the transmitter antenna array as shown in Fig. 7.5. The width of the conductor is less than the width of the microstrip. Also, there is 0.5 mm of air between the coaxial part and the board edge. There are marks filed on the connector top legs which can be

broken halfway or fully for tuning the connector interface. Therefore, upon testing the manufactured antenna, the measured output may be different to the results of the simulation.
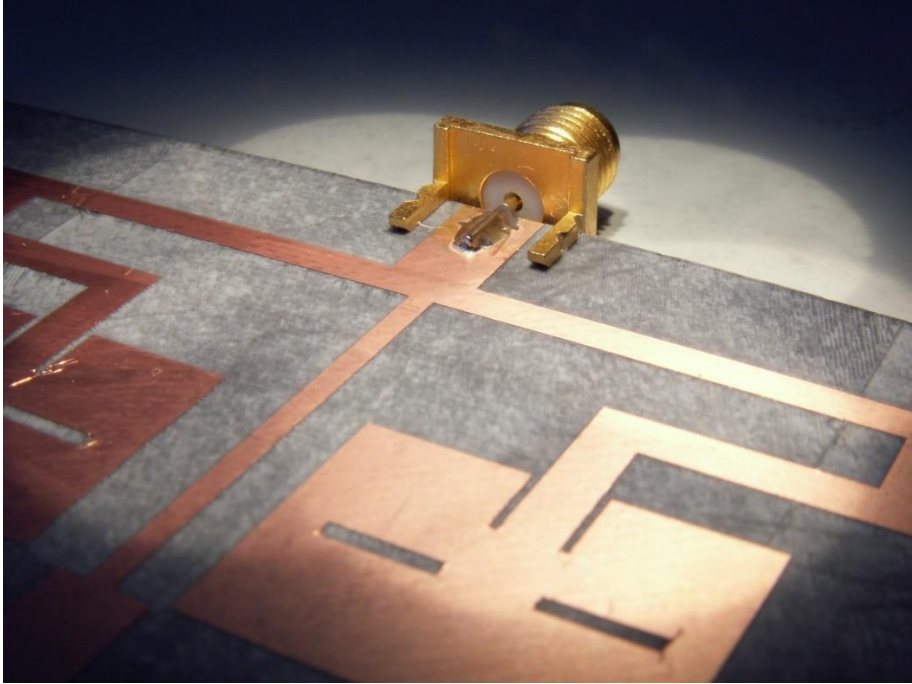
Figure 7.5: SMA connector mounted on the transmitter antenna array.

Chapter 8

Conclusion and Future Work

The aim of the thesis is to design an antenna array for a harmonic radar application used to monitor Bogong moth in the Australian Alps. The main challenge was to increase the bandwidth and reduce the coupling between the transmitter and receiver antenna arrays. The other challenges like choosing the permittivity and designing the array within the given dimension 200×300mm for the arrays to be placed also plays a major role. The required gain of the antenna for transmitter is 20dBi and receiver is 26dBi. On calculating the maximum directivity theoretically in Chapter 5 (Section 5.4), we found the maximum directivity for transmitter antenna to be 16dB and receiver antenna to be 17.24dB. From the simulation we got an output of 14.8dBi ≈ 15dBi gain at the transmitter and 15.7dBi ≈ 16dBi at the receiver array. Also, we found the aperture efficiency to be 0.79 for the transmitter antenna and 0.75 for the receiver antenna array. According to the planar array the aperture efficiency should be between 0.6 to 0.8. We also achieved good matching with impedance, VSWR, and reflection coefficient. The simulations were done for the different antenna array designs and the best ones to fit the requirements were approved as final. We were working on bandwidth such that the VSWR value to be lesser than 1.5 so that we can cover a larger bandwidth while 50MHz was expected. There was previous work carried out on the same subject area but now our thesis is done at ISM band to work in an unlicensed spectrum.

Thus, except for the directivity, we have met the requirements for the project. However, if we had more time to work on the project, then we would think of designing a radome for the antenna to be able to work in different climatic conditions. Moreover, we would like to understand the properties of different connectors that are used in the inset feed. This is because in our project we have designed the antenna, but the connecting port is an edge port in the FEKO software. In contrast, in real

implementation we need to choose a real connector and the type of connectors used needs to be calibrated to offer the same results as we obtained from simulation. Also, there are different ways to design the layout of the antenna arrays, one way is to put the transmitter array on top of the receiver array, and the other is to mount both antenna arrays beside each other. It would be interesting to investigate both array layouts, with the aim to achieve better gain with less coupling between the antenna arrays.

References

[1] S. Maci and G. Bifji Gentili, *"Dual-Frequency Patch Antennas"*, in IEEE Antennas and Propagation Magazine, Vol. 39, No. 6, December 1997.

[2] George Hardesty, "*Antenna Beamwidth*". Blog Post, 11 October 2019. Available: https://www.data-alliance.net/blog/antenna-beamwidth/.

[3] Wikipedia contributors. (2020, February 22). Beamwidth. In *Wikipedia, The Free Encyclopedia*. Retrieved 14:05, 7 August 2021. Available: https://en.wikipedia.org/w/index.php?title=Beamwidth&oldid=9 42024483.

[4] Virgilio Zúñiga, N. Haridas, A. Erdogan, and T. Arslan, *"Effect of a Central Antenna Element on the Directivity, Half-Power Beamwidth and Side-Lobe Level of Circular Antenna Arrays"*, in NASA/ESA Conference on Adaptive Hardware and Systems, 29 July 2009.

[5] Liton Chandra Paul, Md. Sarwar Hosain, Sohag Sarker, Makhluk Hossain Prio, Monir Morshed and Ajay Krishno Sarkar, "*The Effect of Changing Substrate Material and Thickness on the Performance of Inset Feed Micro strip Patch Antenna",* in American Journal of Networks and Communications, Vol. 4, No.3, Pages 54-58, Published online May12, 2015.

[6] Ze Fu and Hamza Bin Faheem, "*Compact and Lightweight Antenna Designs for Harmonic Radar Application"*, in master's thesis, Department of Electrical and Information Technology, Lund University, Sweden, September 30, 2018.

[7] Amit Kumar, Jaspreet Kaur and Rajinder Singh, "*Performance Analysis of Different Feeding Techniques",* in International Journal of Emerging Technology and Advanced Engineering, Vol. 3, Issue 3, Pages 884-890, March 2013.

[8] Youssef Rhazi, Seddik Bri and Rajaa Touahani, *"Effect of Microstrip Antenna Feeding in the K-band"*, in International Journal of Engineering and Technology (IJET), Vol 4, No. 6, Pages 515-522, December 2012-January 2013.

[9] Charles U. Ndujiuba and Adetokunbo O. Oloyede, *"Selecting Best Feeding Technique of a Rectangular Patch Antenna for an Application"*, in International Journal of Electromagnetics and Applications, Vol. 5, No. 3, Pages 99-107, 2015.

[10] Sonia Sharma, C. C. Tripathi and Rahul Rishi, *"Impedance Matching Techniques for Microstrip Patch Antenna",* in Indian Journal of Science and Technology, Vol. 10, No. 28, Pages 1-16, July 2017.

[11] Akaninyene B. Obot, Gabriel A. Igwue, and Kufre M. Udofia, *"Design and Simulation of Rectangular Microstrip Antenna Arrays for Improved Gain Performance",* in International Journal of Networks and Communications, Vol. 9, No. 2, Pages 73-81, 2019.

[12] Constantine A. Balanis, "*Antenna Theory, Analysis and Design*" 3rd Edition, 2005.

[13] Saleh A. Aljaser, "*Miniaturization of a Low Power Harmonic Radar for UAV use*"*,* in master's thesis, Department of Electrical and Information Technology, Lund University, Sweden, 14 June 2019.

[14] John Merbin, M. Ayyappan, B. Manoj and Stephen Rodrigues, *"Bandwidth Enhancement of Microstrip Patch Antenna for 5.8GHz by Optimized Feed Offset*", in International Conference on Communication and Signal Processing, 6-8 April 2016, India.

[15] Rogers antenna substrate, https://rogerscorp.com//media/project/rogerscorp/documents/advanced-connectivitysolutions/english/data-sheets/rt-duroid-5870---5880-data-sheet.pdf.

[16] "*Bandwidth of an Antenna"*. Available: https://www.mobilemark.com/about/faq/how-do-you-specify-the-bandwidth-of-an-antenna/.

[17] Wikipedia contributors, *"Antenna array*", in Wikipedia, The Free Encyclopedia, 5 November 2021 Retrieved 12:40, 15 December 2021,

Available: https://en.wikipedia.org/w/index.php?title=Antenna_array&oldid=1053730557.

[18] Hamid Mubarak and Mustafa Makkawi, "*Performance Evaluation of 1×2 Patch Antenna Array based on Power Divider Characterises*", Pages 6-12, 20-23 February 2016, Conference of Basic Sciences and Engineering Studies (SGCAC), DOI: 10.1109/ SGCAC.2016.7457998.

[19] Kufre M. Udofia and Jeffrey C. Saturday, "*Parametric Comparison of Circular, Triangular and Rectangular Dual-Band Microstrip Antenna for Wireless Communication*", in European Journal of Engineering and Technology, Vol. 7, No. 3, Pages 9-20, 2019.

[20] Md. Tanvir Ishtaique-ul Huque, Md. Kamal Hosain, Md. Shihabul Islam, and Md. Al Amin Chowdhury, "*Design and Performance Analysis of Microstrip Array Antennas with Optimum Parameters for X-band Applications",* in (IJACSA) International Journal of Advanced Computer Science and Applications, Vol. 2, No. 4, Pages 81-87, 2011.

[21] G. J. K. Moernaut and D. Orban*, "The Basics of Antenna Arrays*", from Orban Microwave Products. Available: http://www.orbanmicrowave.com.

[22] Zhigang Xiao, Jiang Yao, and Shaoquan Yin, *"High Directivity Antenna Array Based on Artificial Electromagnetic Metamaterials with Low Refractive Index"* in International Journal of Antennas and Propagation, Volume 2015, Article ID 294598.

MATLAB Code

Calculating the antenna parameters:

```matlab
clear;
close all;
clc;

%%%%INPUTS
disp('Enter known parameters:');
er = input('Enter the permittivity');
h = input('Enter height of substrate (mm)');
f = input('Enter target frequency (GHz)');
z0 = input('Enter input impedance z0 (ohms)');
disp('Calculating...');
c = 3e8;

%%%%CALCULATIONS

% HEIGHT
h = h*1e-3;
% FREQ
f = f*1e9;
% LAMBDA
lambda = c/f;

%%% WIDTH OF PATCH
wp = (c/(2*f))*(sqrt(2/(er+1))); % 4.2

%%% EFFECTIVE PERMITTIVITY
ereff = ((er+1)/2) + (((er-
1)/(2*sqrt(1/(1+((12*h)/wp))))));

%%% EFFECTIVE LENGTH
Leff = (c/(2*f*sqrt(ereff)));
```

```matlab
%%% CALCULATION OF THE PATCH LENGTH EXTENSION dLENGTH
dL = ((0.412*h)*(ereff+0.3)*((wp/h)+(0.26)))/((ereff-
0.258)*((wp/h)+0.8));

%%% LENGTH OF PATCH
LP = Leff-(2*dL);

%%% WIDTH OF SUBSTRATE
ws = wp + (6*h);

%%% LENGTH OF SUBSTRATE
ls = LP + (6*h);

%%% CALCULATING THE RESONANT INPUT EDGE RESISTANCE (RIN)
OF THE PATCH
k = (2*pi)/lambda;
x = k*wp;
i1 = -2 + cos(x)+(x*sinint(x)) + (sin(x)/x);
G1 = i1/(120*pi*pi);

%%% CONDUCTANCE 2
a = @(th)
(((sin((x./2).*cos(th))./cos(th)).^2).*(besselj(0,(k.*LP
.*sin(th)))).*(sin(th)).^3);
a1 = integral(a,0,pi);
G12 = a1/(120*pi*pi);

%%% INPUT IMPEDANCE AT THE LEADING RADIATING EDGE OF THE
PATCH
R_in = 1/(2*(G1+G12));

%%% DETERMINATION OF THE INSET FEED DEPTH Y0
Y0 = ((LP/pi)*acos(sqrt(z0/R_in))) ;

zq = sqrt(z0*R_in);
z=zq;
z1=z-1;

%%% CALCULATION OF WF
for w= 1.0000e-05:0.50000e-05 : 10
w3 = (120*pi)/(sqrt(ereff)*((w/h)+1.393+(
0.6667*log10((w/h)+1.444))));
    if (( round(w3)>=z1 && round(w3)<=z))
        wf =w;
    end
```

```matlab
 end

Zedge= 90* (er^2/(er+1))*(LP/wp) ;

%%% CALCULATION OF THE INSET (FEED):
fl = 3*h ;

%%% QUARTER WAVE LENGTH
yg = lambda/(sqrt(ereff));

%%% FEED LENGTH
QuarterWaveLenby4 = yg/4;

%%% QUARTER FEED WIDTH
disp('Rectangle Patch');
disp(['Patch Width:',num2str(wp*(1e3)), ' mm']);
disp(['Patch Length:',num2str(LP*(1e3)), ' mm']);
disp('Input impedance using Inset feed length ');
disp(['YO:',num2str(Y0*(1e3)), ' mm']);
disp(['wf:',num2str(wf*(1e3)), ' mm']);
disp(['fl:',num2str(fl*(1e3)), ' mm']);
disp('Input impedance using Quarter wave tranformation
');
disp(['QuarterWaveLenby4:',num2str(QuarterWaveLenby4*(1e
3)), ' mm']);
```